



**US Army Corps
of Engineers**

Construction Engineering
Research Laboratories

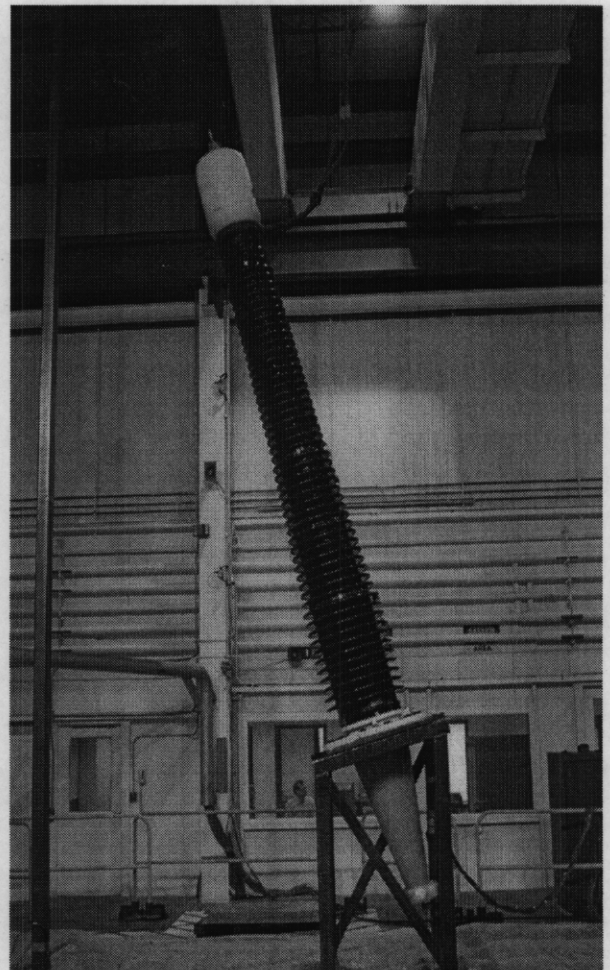
USACERL Technical Report 97/57
February 1997

Fragility Testing of a Power Transformer Bushing

Demonstration of CERL Equipment Fragility and Protection Procedure

by
James Wilcoski and Steven J. Smith

This report presents a demonstration of the CERL Equipment Fragility and Protection Procedure (CEFAPP) as used in the testing of a large power transformer bushing. CEFAPP defines the capacity of critical equipment by tests conducted on a shake table. Equipment capacity is defined in terms of amplitude of motions with respect to frequency that cause equipment failure. These spectral amplitudes can be defined in terms of either response spectrum or support motion spectral amplitude, both plotted with respect to frequency. Equipment failure may be loss of function, physical damage or some measured response that is determined by the test engineer to be unacceptably high. The bushing failure mode defined in this application was leaking and slippage at the porcelain/flange interface. The equipment capacity as defined by this failure envelope is later compared with the demand as defined by the user design spectra. This demand may be site specific or code based response spectra or spectral motions at equipment installation location based on a detailed numerical analysis of the building in which the equipment is to be installed. For the bushing presented here, capacity is defined in terms of response spectrum of the shake table support motions that can be compared with site-specific response spectra or design response spectra based on IEEE 693. Technical details of CEFAPP may be found in a companion report, USACERL Technical Report 97/58.



REPORT DOCUMENTATION PAGE

Form Approved
OMB No. 0704-0188

Public reporting burden for this collection of information is estimated to average 1 hour per response, including the time for reviewing instructions, searching existing data sources, gathering and maintaining the data needed, and completing and reviewing the collection of information. Send comments regarding this burden estimate or any other aspect of this collection of information, including suggestions for reducing this burden, to Washington Headquarters Services, Directorate for Information Operations and Reports, 1215 Jefferson Davis Highway, Suite 1204, Arlington, VA 22202-4302, and to the Office of Management and Budget, Paperwork Reduction Project (0704-0188), Washington, DC 20503.

1. AGENCY USE ONLY (Leave Blank)	2. REPORT DATE February 1997	3. REPORT TYPE AND DATES COVERED Final	
4. TITLE AND SUBTITLE Fragility Testing of a Power Transformer Bushing		5. FUNDING NUMBERS 4A162784 AT41 CA7	
6. AUTHOR(S) James Wilcoski and Steven J. Smith			
7. PERFORMING ORGANIZATION NAME(S) AND ADDRESS(ES) U.S. Army Construction Engineering Research Laboratories (USACERL) P.O. Box 9005 Champaign, IL 61826-9005		8. PERFORMING ORGANIZATION REPORT NUMBER TR 97/57	
9. SPONSORING / MONITORING AGENCY NAME(S) AND ADDRESS(ES) HQ USACE ATTN: CEMP-ET 20 Massachusetts Ave. NW Washington, DC 20314-1000		10. SPONSORING / MONITORING AGENCY REPORT NUMBER	
11. SUPPLEMENTARY NOTES Copies are available from the National Technical Information Service, 5285 Port Royal Road, Springfield, VA 22161.			
12a. DISTRIBUTION / AVAILABILITY STATEMENT Approved for public release; distribution is unlimited.		12b. DISTRIBUTION CODE	
13. ABSTRACT (Maximum 200 words) <p>This report presents a demonstration of the CERL Equipment Fragility and Protection Procedure (CEFAPP) as used in the testing of a large power transformer bushing. CEFAPP defines the capacity of critical equipment by tests conducted on a shake table. Equipment capacity is defined in terms of amplitude of motions with respect to frequency that cause equipment failure. These spectral amplitudes can be defined in terms of either response spectrum or support motion spectral amplitude, both plotted with respect to frequency. Equipment failure may comprise loss of function, physical damage, or some measured response that is determined by the test engineer to be unacceptably high. The bushing failure mode defined in this application was leaking and slippage at the porcelain/flange interface. The equipment capacity as defined by this failure envelope is later compared with the demand as defined by the user design spectra. This demand may be site-specific or code based response spectra, or spectral motions at equipment installation location based on a detailed numerical analysis of the building in which the equipment is to be installed. For the bushing presented here, capacity is defined in terms of response spectrum of the shake table support motions that can be compared with site-specific response spectra or design response spectra based on IEEE 693. Technical details of CEFAPP may be found in a companion report, USACERL Technical Report 97/58.</p>			
14. SUBJECT TERMS Seismic vulnerability Equipment evaluation Transformer		15. NUMBER OF PAGES 62	16. PRICE CODE
17. SECURITY CLASSIFICATION OF REPORT Unclassified	18. SECURITY CLASSIFICATION OF THIS PAGE Unclassified	19. SECURITY CLASSIFICATION OF ABSTRACT Unclassified	20. LIMITATION OF ABSTRACT SAR

Foreword

This study was conducted for Headquarters, U.S. Army Corps of Engineers under Project 4A162784AT41, "Military Facilities Engineering Technology"; Work Unit CA7, "Seismic Protection of Equipment." The technical monitor was Charles Gutberlet, CEMP-ET.

The work was performed by the Engineering Division (FL-E) of the Facilities Technology Laboratory (FL), U.S. Army Construction Engineering Research Laboratories (USACERL). The USACERL Principal Investigator was James Wilcoski. Larry M. Windingland is Acting Chief, CECER-FL-E, and Donald F. Fournier is Acting Operations Chief, CECER-FL. The USACERL technical editor was Gordon L. Cohen, Technical Information Team.

The authors acknowledge the work of James B. Gambill, who operates the USACERL Triaxial Earthquake and Shock Simulator (TESS). Mr. Gambill installed instrumentation, and set up and ran all bushing tests.

USACERL gratefully acknowledges the Tennessee Valley Authority (TVA) for allowing USACERL to perform fragility testing on a TVA power transformer bushing. The use of this bushing provided an opportunity to demonstrate the test procedure on critical equipment that may be vulnerable to seismic motions. Further information about the seismic behavior of this bushing is available in the TVA report "Earthquake Analysis and Shake Table Seismic Testing of 500 kV Transformer Bushing/Bus Bar Configuration Used at TVA Electric Substations," by Husein A. Hasan and Joe V. Peyton (December 13, 1996). Mr. Hasan and Mr. Peyton are members of the Resource Group/Engineering Services at TVA.

COL James A. Walter is Commander of USACERL, and Dr. Michael J. O'Connor is Director.

Contents

SF 298	1
Foreword	2
List of Tables and Figures	4
1 Introduction	7
Background	7
Objective	8
Approach	9
Scope	9
Mode of Technology Transfer	10
2 Fragility Testing Procedure	11
Seismic Design Response Spectra	11
Generating Narrow-Band Random Records	11
Scaling the Narrow-Band Random Records	13
Documenting Failures Based on Response Spectra Amplitude	18
Probability Considerations for Fragility Data	21
Using the Fragility Data	23
3 Conclusions	24
Figures Referenced in Main Body of Report	25
Appendix: Matlab Routine for Generating Narrow-Band Random Sweep Records	55
Distribution	

List of Tables and Figures

Tables

1	Narrow-band random signal generation Matlab program parameters	13
2	Scaling relationships for narrow-band random records	15
3	Amplitude of tests conducted on the TESS, percent of Figure 7 records	16
4	Bushing primary modes of vibration and associated damping	18
5	Qualification tests conducted on the TESS, percent IEEE 693 HP Level & TVA Site-Specific	20

Figures

1	TVA power transformer bushing tested on the USACERL TESS	26
2	Horizontal and vertical response spectra, high seismic performance level, IEEE 693	27
3a	Generated narrow-band random signal, Ran1	27
3b	Generated narrow-band random signal, Ran2	28
3c	Generated narrow-band random signal, Ran3	28
3d	Generated narrow-band random signal, Ran4	28
3e	Generated narrow-band random signal, Ran5	29
3f	Generated narrow-band random signal, Ran6	29
3g	Generated narrow-band random signal, Ran7	29
3h	Generated narrow-band random signal, Ran8	30

3i	Generated narrow-band random signal, Ran9	30
3j	Generated narrow-band random signal, Ran10	30
4	IEEE 693 high seismic performance response spectra and unscaled response spectra	31
5	Scaling used for both horizontal (lateral and longitudinal) and vertical records ..	32
6a	IEEE 693 high seismic performance response spectra and scaled response spectra	33
6b	IEEE 693 spectra and selected scaled response spectra	33
7a	Lateral narrow-band random scaled signal, Ran 8	35
7b	Longitudinal narrow-band random scaled signal, Ran3	35
7c	Vertical narrow-band random scaled signal, Ran9	36
8a	Achieved lateral acceleration with input motions at 29% of Figure 7a	36
8b	Achieved longitudinal acceleration with input motions at 29% of Figure 7b	37
8c	Achieved vertical acceleration with input motions at 29% of Figure 7c	37
9	Test response spectra from 29% Figure 7 motions and 29% IEEE 693 Spectra ..	39
10a	Achieved lateral acceleration, 50% of Figure 7a (Frag10)	39
10b	Achieved longitudinal acceleration, 50% of Figure 7b with 1.2 Hz HP filter	41
10c	Achieved vertical acceleration, 50% of Figure 7c	41
11a	Scale with Notch 2	42
11b	Lateral achieved acceleration with Notch 2 and 100% of Figure 7a (Frag17) ...	42
11c	Longitudinal achieved acceleration with Notch 2, 100% of Figure 7b (Frag 17) .	42
11d	Vertical achieved acceleration with Notch 2 and 100% of Figure 7c (Frag17) ...	43
11e	IEEE 693 spectra and TSR for 100% of Fig. 7 motions with Notch 2 (Frag17) ..	43

12a	Scale and Notch 1	45
12b	Scale and Notch 2	45
12c	Scale and Notch 3	45
13a	Maximum TRS through Frag23, 220% of Figure 7	47
13b	Maximum TRS through Frag23 and failure data	47
13c	Maximum TRS without notches	49
14a	IEEE 693 (at 50% PL) and site-specific spectra, TRS, and leak failures	49
14b	Failure data from CEFAPP, IEEE 693, and site-specific tests	51
15	Acceleration power spectral density plots, longitudinal for 160% of Figure 7 ...	51
16	Fragility data with site-specific and IEEE 693 design response spectrum	53

1 Introduction

Background

Earthquakes often cause more costly damage to building contents than to the buildings themselves,* and significant costs are associated with the loss of function of critical equipment. Equipment damage can be significantly reduced by ensuring adequate anchorage, bracing, and “rattle space.” However, sensitive equipment with this protection has failed in even moderate earthquakes, because the equipment itself lacks sufficient strength.

The U.S. Army Construction Engineering Research Laboratories (USACERL) has developed a new shake table test procedure for defining the vulnerability of critical equipment. The CERL Equipment Fragility and Protection Procedure (CEFAPP) defines the capacity of equipment to withstand transient support motions in terms of amplitude versus frequency. The amplitude in this application is response spectrum values at which failure occurs. Failure may be actual mechanical damage, temporary loss of function, acceleration or strain levels at critical locations or any other criteria defined by the test engineer. The frequency content of support motion is critical as it determines the manner (modes) in which equipment responds and fails. The amplitude, frequency, and mode of failure are recorded as single data points for each failure. Multiple equipment failure data points are plotted on a frequency axis, creating a failure envelope that defines the equipment capacity.

Design engineers evaluating the installation of equipment can define predicted motions at equipment installation locations in terms of design response spectrum. These spectra, defining the demand, are overlaid against experimentally defined equipment capacity plots to evaluate the adequacy of equipment. Any number of demand environments (design spectra) may be compared against the experimentally defined capacity without need for further expensive - and often over conservative - qualification testing. Equipment manufacturers can use CEFAPP as a design aid, because the test results define improvements needed to withstand a variety of

* Federal Emergency Management Agency (FEMA) 74, *Reducing the Risks of Nonstructural Earthquake Damage* — A Practical Guide, September 1994, pp 7–12.

demands. CEFAPP can also be used as a diagnostic tool to characterize failures that prevent passing qualification tests.

The Tennessee Valley Authority (TVA) conducted seismic qualification tests on a 500 kV Power Transformer Bushing using TESS, the Triaxial Earthquake and Shock Simulator at USACERL.* The bushing sustained no permanent damage in these tests, and TVA donated the bushing to USACERL for fragility testing. The use of this bushing provided an opportunity to demonstrate CEFAPP on critical equipment that may be vulnerable to seismic motions. Figure 1 shows the TVA bushing mounted on the TESS.**

Porcelain power transformer bushings have been particularly vulnerable to earthquakes, with numerous failures reported even in moderate earthquakes. High-voltage bushings (230 kV or larger) have experienced numerous failures in recent earthquakes (1994 Northridge in particular).*** Inertia forces from seismic motions create large bending moments at the porcelain/flange connection, resulting in oil leaks, slippage, and porcelain failure. The porcelain failure is caused by stress concentrations resulting from porcelain contact with the metal flange. Porcelain is very brittle and weak in tension such that high compressive forces at the porcelain/flange surface creates poisson-related hoop tensile stresses, resulting in brittle failures.

Objective

The objective of this study was to demonstrate the application of CEFAPP on a critical equipment item whose vulnerability is of broad concern. The process for defining and using the vulnerability data gathered from this procedure is demonstrated in this report, but the details of vulnerability for the specific equipment tested are not included, as explained under "Scope" below. Reference is made to IEEE 693, which is an equipment qualification procedure. It should be noted that CEFAPP is intended to determine fragility, not qualification.

* This test program and related analysis are summarized in the TVA report "Earthquake Analysis and Shake Table Seismic Testing of 500 kV Transformer Bushing / Bushing Bus Bar Configuration Used at TVA Electric

** Substations," by Husein A. Hasan and Joe V. Peyton, December 13, 1996.

*** All figures have been placed at the end of this report, beginning on page 26.

Guide to Post-Earthquake Investigations of Lifelines, Technical Council on Lifeline Earthquake Engineering of the American Society of Civil Engineers, Monograph No. 3, August 1991, edited by Anshel J. Schiff.

Approach

This report focuses discussion on the development of test waveforms and methods for documenting failures, not details of bushing vulnerability. Limited test results are presented to illustrate the information gained through the test procedure.

The test waveforms are narrow-band random sweep records (see page ? for discussion of narrow band versus broad band). The starting point for defining support motions can be based on design response spectra or some other predetermined spectrum envelope. The example described in this report uses the IEEE* 693 seismic design response spectra as a basis for generating narrow-band random sweep motions. A Matlab** routine was developed to generate these records and the records are scaled to "fit" the IEEE 693 design spectra. Tests are then performed using these records; the amplitudes are increased and failure data are gathered. Then energy is removed in the frequency range of failure by "notching" the records, and the tests are repeated at higher energy levels within the modified spectra. As new failure data are gathered, the failures are documented based on response spectra amplitude and mode of failure. The failure data are validated with site specific and design spectra qualification tests whose results can be compared directly with the failure data. Finally, procedures for using the failure data to define the equipment's seismic vulnerability and to develop methods to protect vulnerable equipment are presented.

Scope

Test data presented here is limited to shake table motions and displacement measurements at the bushing flange interface, because of the potential proprietary nature of the data. Other measured values are not needed to demonstrate CEFAPP. The results of any real-world application of this procedure would present all data, including measurements that may be taken at various locations to define equipment response and modes of failure. Quantifying equipment dynamic characteristics and modes of failure is essential to developing equipment protection. Based on the vulnerability data gathered, analytical models can be developed that would allow the generalization of the vulnerability data to equipment with similar dynamic characteristics and modes of failure. Vulnerability of equipment not tested could be defined based on these models. Such models have not been included in this study.

* IEEE: Institute of Electrical and Electronics Engineers.

** Matlab is a trademark of The MathWorks, Inc., Natick, MA 01760.

Mode of Technology Transfer

The development of this test procedure is documented in the USACERL Technical Report (TR) M-97/58, *CERL Equipment Fragility and Protection Procedure*, by James Wilcoski, J.B. Gambill, and S.J. Smith (USACERL, in press, 1997). This procedure will be presented in a technical journal and an Engineering Technical Letter. The procedure will impact Army Technical Manual (TM) 5-809-10-1, *Seismic Design Guidelines for Essential Buildings*, and U.S. Air Force manual ESL-TR-87-57, *Protective Construction Design Manual* (Air Force Engineering and Services Center, 1989).

2 Fragility Testing Procedure

Seismic Design Response Spectra

Widely accepted design spectra should be used when available for the equipment being tested. The spectra used in this example (Figure 2) are from the Institute of Electrical and Electronics Engineers (IEEE) 693, "Recommended Practices for Seismic Design of Substations" (Draft 6, 1997), Figure 3, "High Seismic Performance Level (PL)" with 2% of critical damping. According to section 9.3.1 IEEE 693, "Equipment that is shown by this practice to perform acceptably in ground shaking up to the High Seismic Performance Level is said to be seismically qualified to the High level." Thus, these spectra provide an industry-recognized starting point for defining the test motions for Electrical Power Substation Equipment. The leakage criteria for bushings (IEEE 693, section D.5.1.d) requires that the bushing gasket not leak when subjected to PL shake table testing that has been adjusted for the influence of the transformer and local flexibility at the bushing mounting. Section D.4.3 of IEEE 693 states that the acceleration levels at the bushing flange can be doubled to account for this amplification of the transformer. Such modification was not applied to the "starting point" spectra, as the fragility data generated could be used for bushings attached to a variety of transformers. The fragility data generated from this test procedure will later be compared with design spectra that should be modified to reflect amplification from the transformer. Testing at the high seismic PLs allows direct comparison with ultimate strength of porcelain or other components. Figure 2 shows design spectra for both the horizontal direction and vertical, which is 80% of the horizontal values (IEEE 693, A.1.1.1).

Generating Narrow-Band Random Records

Tests are conducted with narrow-band random sweep motions. These signals are intended to excite equipment response comparable to that of real seismic motions, with the key parameters being band width and sweep rate. USACERL technical report 97/58 presents the basis for defining these parameters, so as to generate an equivalent number single degree of freedom (SDOF) oscillator strong motion cycles. Based on this work a band width of 1/3rd octave and a sweep rate of 6 octaves per

minute was used in the bushing tests. This creates a random signal with the energy of motion concentrated within prescribed frequency limits, and the center frequency moves at a defined rate with respect to time (6 octaves per minute for the bushing tests). Each octave is a doubling in frequency, so that the center frequency of the records doubles every 10 seconds. At any moment in time the energy of signal is concentrated within 1/3rd octave by offsetting the high and low pass filters 1/6th octave from the center frequency. The 1/3rd octave width will more realistically excite closely spaced modes than sine sweep tests.

The next step in the fragility testing procedure is to generate random motions on the shake table that spans the full frequency range. A Matlab routine called RANSWP.M (see Appendix)* generates a random signal between 0 and Nyquist frequency ($\frac{1}{2}$ sample rate), exceeding the entire range of the spectrum shown in Figure 2.

RANSWP.M is also used to sweep high- and low-pass filters across this random signal at a user-defined rate. Figures 3a through 3j are examples of records (Ran1 through Ran10) generated using this program. The variables used to generate these records are defined as follows:

- **Current Time.** The waveform created by RANSWP is based on pseudo-random numbers generated by Matlab. A default value of zero is used for the random number generator at the beginning of new Matlab sessions. Using this default value would lead to the generation of exactly the same signal for each new session in Matlab. Therefore, the user is prompted to enter the current time, which is used as the starting point of the random number generation. The time is formatted as hr.min (e.g., 11.21 for 11:21 a.m.).
- **Sample Rate.** This is the frequency at which data points are generated (inverse of time step) in the digitized record. Experience (see Otenes and Enachson 1972) indicates that 2.5 samples per cycle, or a sample rate of at least 2.5 times the ending frequency, is needed. For the records in Figures 3a through 3j, this becomes (64 Hz + 1/6th octave) x 2.5 = 180 Hz.
- **Sweep Rate.** This is the rate at which the high- and low-pass filters sweep across the random record. The basis for defining this rate is presented in USACERL Technical Report 97/58.

* Subsequent to this application, the routine shown in the Appendix was improved and is presented in Appendix A of USACERL Technical Report 97/58. The quality of the sweeping filters was evaluated in the fourth chapter of this report for both routines.

- Starting Center Frequency.** This defines the lower frequency of interest for which the fragility tests are to be conducted, normally based on the lower frequency limit of the design response spectra. This frequency should be chosen at a conservatively low point recognizing that data may later be needed at lower frequencies than anticipated in the original test program.
- Ending Center Frequency.** This similarly defines the upper frequency of interest, and it also should be chosen at a conservatively high point.
- Filter Band Width.** This is the difference in frequency between the high-pass and low-pass filter at any point in time during the sweep. This variable is defined in terms of octaves (doubling of frequency) and remains constant throughout the record. This variable is held constant at 1/3rd octave for all tests using this procedure, as this width is narrow enough to define the frequency at which failure occurs yet wide enough that the signal remains somewhat random (i.e., not a sine sweep).

Table 1. Narrow-band random signal generation Matlab program parameters.

Parameter	Figure 3a - 3j values
Sample Rate (Hz)	200
Sweep Rate (octaves/min)	6
Starting Center Frequency (Hz)	0.5
Ending Center Frequency (Hz)	64
Filter Band Width (octaves)	0.33333

Table 1 gives the values for these parameters as used to generate the records shown in Figures 3a – 3j.

Scaling the Narrow-Band Random Records

The amplitude of the records shown in Figures 3a – 3j are unitless. They are scaled across their frequency range to produce levels consistent with the baseline design response spectra. This scaling can be illustrated by scaling the records shown in Figures 3a – 3j to produce response spectrum levels consistent with Figure 2. This is done by generating a response spectrum for each record using the same percentage of critical damping used to generate the baseline design response spectra (e.g., 2% for the current example shown in Figure 2). The response spectra are plots of the maximum response of SDOF oscillators subjected to support motions across a frequency range. Response spectra are generated from the unitless records shown in Figures 3a – 3j using the TESS operating software. Input parameters for generating the response spectra include the following:

- **Starting Frequency**, which is normally the same as the Starting Center Frequency defined above.
- **Ending Frequency**, which is normally the same as the Ending Center Frequency defined above.
- **Number of Frequency Points per Octave**, which defines the increment in frequency for the response spectrum calculations, which for the example here is 24, yielding 168 points (SDOF oscillators) across the seven-octave record.
- **Percentage of Critical Damping**, which is the same value used for defining the design response spectra (2% for the current example).

Figure 4 shows the unitless response spectrum plots for each of the narrow-band random records in Figures 3a – 3j, plus the IEEE 693 design spectra from Figure 2. Next, the narrow band records are scaled such that their response spectra become equivalent to the amplitude shown in the design spectra. Figure 4 shows where and to what degree the unitless spectra need to be scaled to produce response spectra equivalent to the design spectra. Table 2 shows frequency ranges and expressions (linear in this example) used to scale the unitless spectra. Figure 5 graphically shows the expressions for scaling the horizontal (lateral and longitudinal) and vertical narrow-band random records. Figure 5 also includes the information from Table 2 to provide direct comparison with the plots in Figure 5. Time for the narrow-band random records is directly related to the center frequency as defined by the sweep rate, with their ranges shown in Table 2. The dual Frequency and Time axis used in Figure 5 illustrates the center frequency and time correspondence. Figure 6a shows the scaled response spectra after multiplying the spectra in Figure 4 by the expressions shown in both Table 2 and Figure 5. The amplitudes of the response spectra in Figure 6a vary greatly from the IEEE 693 design spectrum envelopes. From these records, three are selected that have the smallest variation from the design spectra, and these are used for shake table motions. Each of these records has significant energy across the frequency range of interest. Ran8, Ran3, and Ran9 are used for lateral, longitudinal, and vertical motions, respectively. These selected spectra are plotted in Figure 6b. Ran9 was selected for the vertical record because of its relatively small amplitude at the lower frequencies, so as to avoid the large displacements at low frequencies that would quickly exceed the vertical displacement capacity of the TESS. Earlier modal testing of the equipment revealed a dominant first mode at 6 Hz, particularly in the longitudinal direction. Therefore, Ran3 was selected for the longitudinal direction as it has a somewhat more uniform distribution of energy in this frequency range.

Table 2. Scaling relationships for narrow-band random records.

Frequency Range, $f_{n-1} - f_n$ (Hz)	Time Range $t_{n-1} - t_n$ (seconds)	Scale Number & Amplitude,		Horizontal Scaling, S_H (g)	Vertical Scaling, S_V (g)
		n	A_n (g)		
		0	12		
0.5 - 1.122	0 - 11.67	1	8	$\frac{A_1 - A_0}{t_1 - t_0} (t - t_0) + A_0$	$0.8 S_H$
1.122 - 8	11.67 - 40	2	2	$\frac{A_2 - A_1}{t_2 - t_1} (t - t_1) + A_1$	$0.8 S_H$
8 - 33.903	40 - 60.833	3	0.25	$\frac{A_3 - A_2}{t_3 - t_2} (t - t_2) + A_2$	$0.8 S_H$
33.903 - 64	60.833 - 70	4	0.2	$\frac{A_4 - A_3}{t_4 - t_3} (t - t_3) + A_3$	$0.8 S_H$

Ran8 had a similar response spectrum to that of Ran3, and was selected for the lateral signal.

The expressions in Table 2 are next used to scale the unitless narrow band time histories—Ran8, Ran3, and Ran9 in Figures 3h, 3c, and 3i, respectively—to give those shown in Figures 7a – 7c. The records shown in Figures 7a – 7c are plotted with respect both to time and frequency, again to illustrate the time/center frequency correspondence. Finally, these records are used in actual tests on the shake table, beginning at very low levels. Table 3 shows the percentage amplitude used in preliminary tests on the TESS. Figures 8a – 8c show the achieved TESS motions in the lateral (Y), longitudinal (X), and vertical (Z) directions at 29% of the input motions (Test File Frag9) shown in Figures 7a – 7c. The amplitude of these records are great enough so that the achieved motions are much greater than the noise level measured at the TESS, but still below levels that could cause equipment failure. From these records, test response spectra (TRS)* are generated for each of the three directions. Figure 9 shows the TRS plotted relative to 29% of the IEEE 693 design response spectra to guide further revision of the scaling expressions.

* The TRS are the calculated response spectra that are developed from actual time history motion of the shake table for the particular test conducted and value of damping. These do not need to envelope the design spectra from IEEE 693, as would be the case for IEEE 693 qualification tests. Still, the eventual maximum TRS from fragility tests will exceed the design spectra, unless early failures cause notching of the test records, resulting in reduced TRS in the notch region.

Table 3. Amplitude of tests conducted on the TESS, percent of Figure 7 records.

Date of Test	Test File Name	Test Level, % Fig 7	High Pass (HP) Filter or Notch	Failure or Other Observations
10/11/96	Frag9	29%	-	None
10/17/96	Frag10	50%	1.2 Hz HP- Long only	None
10/23/96	Frag11	50%	1.2 Hz HP- Long only	Fluid leaked from the Bushing South Side at 36 seconds (6.1 Hz) - documented w/dsl LVDT = 0.015"
10/23/96	Frag12 Frag13	60%	1.2 Hz HP Long & Vert	Fluid leaked from both North & South side at 35 sec (5.7 Hz) - 36.8 sec (6.3 Hz), Porcelain Slippage at 35 sec (5.7 Hz) (dst).
10/28/96	Frag14	60%	1.2 Hz HP - all 3 axes, Notch1	None
10/28/96	Frag15	80%	1.2 Hz HP - all 3 axes, Notch1	Fluid leaked from South side at 32.5 seconds (4.8 Hz)
10/28/96	Frag16	80%	1.2 Hz HP - all 3 axes, Notch2	None
10/28/96	Frag17	100%	1.2 Hz HP - all 3 axes, Notch2	None
10/28/96	Frag18	120%	HP 1.2 Hz Lat. & Long., 1.8 Hz Vert., Notch2	None
10/29/96	Frag19	140%	HP 1.2 Hz Lat. & Long., 1.8 Hz Vert., Notch2	None
10/29/96	Frag20	160%	HP 1.2 Hz Lat. & Long., 1.8 Hz Vert., Notch2	Fluid leaked at 39 seconds (7.55 Hz)
10/29/96	Frag21	180%	HP 1.2 Hz Lat. & Long., 1.8 Hz Vert., Notch2	Fluid leaked at 30 seconds (4.0 Hz) and 39 seconds (7.55 Hz)
10/30/96	Frag22	200%	HP 1.2 Hz Lat. & Long., 1.8 Hz Vert., Notch3	None
10/30/96	Frag23	220%	HP 1.2 Hz Lat., 1.5 Hz Long. & 1.8 Hz Vert., Notch3	Fluid leaked at 22 seconds (2.3 Hz), dsl & dtx show that 2.3 Hz table motion excites the 6 Hz bushing rocking mode.
10/30/96	Frag24	80%	1.2 Hz HP 3 axes	Greater leaks at 32.5 seconds (2.3 Hz)
10/30/96	Frag25	100%	1.2Hz HP 3 axes	Major leaking and dst = 0.018" slip at 35 seconds (5.6 Hz)
10/31/96	Frag26	120%	HP 1.2 Hz Lat& Long, 1.8 Hz Vert	Major leaking and dst = 0.015" slip at 35 seconds (5.6 Hz) and 0.03" slip at 37.5 seconds (6.7 Hz).
10/31/96	Frag27	140%	HP 1.2 Hz Lat& Long, 1.8 Hz Vert	Major leaking
10/31/96	Frag28	160%	HP 1.2 Hz Lat& Long, 1.8 Hz Vert	Major leaking and det = 0.03" slip at 33 sec (4.9 Hz), dst = 0.01" slip at 35.8 sec (6.0 Hz) and 0.015" at 37.5 sec. (6.7 Hz).

NOTES: dsl = displacement at the south side of bushing along the longitudinal direction; dst = displacement at the south side of bushing along the transverse direction; dtx = TESS longitudinal displacement; det = displacement at east side of bushing along the transverse direction; LVDT = linear variable differential transformer sensor.

The expressions shown in Table 2 may be revised based on the achieved motions so future tests will more closely follow the ideal design spectra. Then the input motions of Figures 7a – 7c are adjusted by the revised expressions. In this example, these expressions were not revised because the TRS matched the design response spectra (see Figure 9).

These records are gradually increased until failures occur. After failures occur, the input signals are notched* using revisions of the scaling expressions shown in Table 2, and the amplitudes of subsequent tests are increased to cause failures at other frequencies. In a similar manner the signals and expressions in Table 2 may be revised to avoid exceeding the shake table motion limits. Alternatively, the driving signals in Figure 7 may be reduced by filtering these records. Table 3 (test file name Frag10) shows that the longitudinal motion in Figure 7b was filtered with a 1.2 Hz high pass (HP) filter to avoid exceeding the longitudinal displacement limits of the TESS. An HP filter removes energy in the signal below the chosen frequency. The resulting decrease in achieved acceleration is reflected in a reduction of the TRS. Figures 10a – 10c show the achieved TESS motions at 50% of Figures 7a – 7c, but with the longitudinal motion of 7b filtered at 1.2 Hz.

Figure 11a shows the scale and notch (Notch 2) for Fragility Test Frag17, which used 100% of the Figure 7 motions. To scale the record, Notch 2 slopes down from 100% of the original levels at 4.49 Hz to 1% at 4.62 Hz, remains constant at 1% to 6.92 Hz and slopes back up to 100% at 7.13 Hz. Figures 11b – 11d show the achieved TESS acceleration in the lateral, longitudinal, and vertical directions, illustrating the effect of the notch in the time domain. Figure 11e shows the TRS generated from these motions; the TRS showing the effectiveness of the notch in reducing shake table motions within the desired frequency range by scaling the time history input motions**. Note that further improvements would be seen if the new Matlab routine had been used for signal generation. Figure 11e also includes IEEE 693 spectra for comparison with the TRS. Figures 12a – 12c are Notches 1 through 3, which were used in the fragility tests as indicated in Table 3.

* Notching is the process of removing energy from these records in the frequency range where multiple failures have already taken place. This is done by multiplying the input motions (Figures 7a - 7c) by revised scaling expressions that include attenuation functions for reducing motions in the time region that corresponds to the frequency range that caused failures. An example is shown in Figures 11a – 11e.

** The effectiveness of the notches in removing energy within a particular frequency range is dependent on the quality of the filters used in the signal generation routine. The quality of the routine used in the bushing test and the improved routine was examined in USACERL technical report 97/58.

Documenting Failures Based on Response Spectra Amplitude

The modal frequency and equivalent viscous damping should be measured for each significant equipment mode of vibration. This basic information is needed to understand the response of the equipment to support motions. The primary bushing modes of vibration (lateral and longitudinal) and associated damping are given in Table 4. The damping values were calculated from the half-power bandwidth of the acceleration transfer functions between the TESS and the top of the bushing, based on low-level sine-sweep tests. The second modes of the bushing are near 30 Hz and are much less significant than the primary modes shown in Table 4. However, other types of equipment may have higher modes that do contribute significantly to the dynamic response of equipment.

For each failure, the time of failure is recorded and the center frequency of motion at that time is determined. The maximum response of an SDOF oscillator at that frequency is calculated, which is the amplitude of the TRS (e.g., Figure 9) at the frequency of failure. This value of response spectrum amplitude, together with the frequency of failure, becomes a failure data point. These same values for each failure are plotted to produce a failure envelope. This failure envelope can now be compared directly with site-specific spectra or design spectra, as they represent the response of SDOF oscillators across a spectrum with the same damping (2% of critical damping in this example).

Normally, fragility tests will be uniaxial and the same tests may be repeated in all three axes. However, for the IEEE 693 guidelines, tests are to be triaxial, with the horizontal design response spectrum shown in Figure 2 applied in both the lateral and longitudinal direction, plus the vertical design spectrum applied vertically. Three independent random signals are needed for the tests to be truly triaxial. Because the test motions in each of the three directions are unique, the TRS will also differ, and the test engineer must determine which amplitude from the three TRS is the dominant cause of failure. Normally this will be the direction of motion that causes amplified equipment response at the frequency of failure.

Table 4. Bushing primary modes of vibration and associated damping.

Mode of Vibration	Natural Frequency (Hz)	Equivalent Viscous Damping (% Critical)
1st Longitudinal	5.66	2.5
1st Lateral	6.35	3.0

Figure 13a shows the maximum achieved response spectra for all fragility tests up through Frag23, along with the IEEE 693 design spectra. The amplitude of these tests went as high as 220% of Figure 7, but with a large notch around the natural frequency of the bushing. Figure 13b shows all the failure points, the same maximum achieved TRS and the IEEE 693 design spectra. The failures are summarized in Table 3. Each failure is either visible fluid leakage or slippage at the porcelain/flange connection*. Note the V-shaped plot of the failures, with the amplitude of motions that cause failure increasing with distance away from the bushing natural frequency. This V-shape will be steeper for equipment with low damping due to the sharpness of resonance. After pushing the test levels very high outside the notch region (to 220% of Figure 7 motions), further tests were conducted with the notch removed. The tests without notches caused increased leakage and slippage, but no additional failure modes were observed. The notchless tests were conducted up to 160% of Figure 7 (Frag 24 – Frag 28). The maximum achieved TRS for these tests can be seen in Figure 13c, along with the IEEE 693 design spectra.

The fragility data presented in Figure 13b can be compared with design response spectra or site-specific spectra to evaluate the equipment's (the bushing's) vulnerability to other support motion. This use of the fragility data was evaluated by testing the bushing according to the IEEE 693 High Performance Level Spectra and particular site-specific spectra. Figure 14a shows the maximum achieved TRS for IEEE 693 random tests. The TESS motions were generated by the shake table software to fit the High Performance Level spectra, with 20 seconds of strong motion and 5 seconds of ramp-up and ramp-down. The TRS shown in Figure 14a are based on 50% of the generated test motions, and the IEEE 693 spectra envelopes are plotted at the same 50%. The test levels were reduced to 32%, at which level leaking was first observed. The TRS amplitude at the 6 Hz natural frequency of the bushing (i.e., response of an SDOF oscillator at 6 Hz) was 1.28 g. This data point is shown in Figure 14a. Table 5 summarizes these tests.

The IEEE 693 tests require random motions with energy across a broad frequency range (see Figure 14a). Random motions tests such as these are necessary in conjunction with fragility tests to confirm that high- and low-frequency modes do not couple together to produce a mode of failure that would not be seen in the

* IEEE 693, Section D.5.1 qualification test acceptance criteria states there shall be no evidence of damage, such as broken, shifted or dislodged insulators, visible leakage of oil, or broken support flanges. The visible fluid leaks and shifting seen at the bushing porcelain/flange connection therefore constitute a type of failure, even though the leaks or minor slippage will not themselves impair bushing performance in the field. The bushing tested at USACERL was filled with 75 gallons of water to represent the weight of oil - had it been filled with oil, the leakage would have lubricated the connection and the slippage may have been much worse leading to gasket or porcelain failure.

Table 5. Qualification tests conducted on the TESS, percent IEEE 693 HP Level & TVA Site-Specific.

Date of Test	Test File Name	Test Level, %Fig 2	High Pass (HP) Filter	Failure or Other Observations
10/29/96	IEEE2	20%	None	None
10/29/96	IEEE3	30%	1.0 Hz HP- Long only	None
10/29/96	IEEE4	50%	1.0 Hz HP all 3 axes	Major fluid leaks
10/29/96	IEEE5	40%	1.0 Hz HP all 3 axes	Moderate fluid leaks
10/30/96	IEEE6	35%	1.0 Hz HP all 3 axes	Small leaks
10/30/96	IEEE7	32%	HP 1.0 Hz Long & Vert	Small leak
10/29/96	EQTST31*	200%	None	Site-specific spectra; small leak

*The test level of EQTST31 was 200% the time-histories generated to fit the TVA site-specific spectra.

sweeping narrow-band random fragility tests. Thus these tests validate that coupled modes have not been overlooked in the fragility test procedure.

In a similar manner, the bushing was tested against time-histories generated to fit TVA site-specific spectra. Leaking was first initiated at 200% of these motions, and the resulting TRS is plotted in Figure 14a. The amplitude of the TRS at 6 Hz for the site-specific spectrum-based test was slightly greater at 1.61 g. This is because the dominant energy for the site-specific waveform peaks at slightly greater frequencies than the 6 Hz bushing frequency, where IEEE 693 specifies a broad distribution of energy across the spectrum. Table 5 also summarizes the site-specific test.

The magnitude of the TRS at failure and at 6 Hz, from both the IEEE 693 and site-specific tests, agree well with the magnitude of failure in the fragility tests at 6 Hz. Figure 14b shows the failure points from the fragility, IEEE 693, and site-specific tests. However, the fragility tests reveal more information in terms of the equipment's vulnerability to motions away from its own natural frequency—the sharpness of the V, for example, in Figure 13b. Test data from Frag23 suggest that 2.3 Hz motions excited a 6 Hz (first mode) response in the bushing. This observation is based on comparing the TESS achieved acceleration and longitudinal (axis of bushing) displacement from a linear variable differential transformer (LVDT) sensor around 22 seconds.

Several observations can be made from acceleration power spectral density (APSD) plots. Figure 15 is such a plot (longitudinal motions only) for tests Frag20 and

Frag28 (see Table 3 for test definitions). Frag20 uses support motion scaled at 160% of Figure 7, but with energy removed near the bushing natural frequency using Notch 2. The frequency range of Notch 2 is described earlier in this report. Frag28 uses the same 160% of Figure 7 motions, but with no notching. Figure 15 shows that the table motion energy for these two tests remains the same away from the notch (i.e., comparing TESS w/Notch 2 versus TESS No Notch). Comparing these tests also shows the effect of the notching on the energy in the notch region. The APSD plots for the top of the bushing reveal that the notch does reduce the response at the top of the bushing throughout the notch region. However, between 5 and 6 Hz (very close to the bushing frequency) the top of the bushing APSD is almost as great with the notch as without. This demonstrates that either (1) motions at frequencies outside of the notch region or (2) the limited TESS motions at 6 Hz are exciting the 6 Hz rocking mode of the bushing. The test data could be analyzed further to evaluate the response of the bushing, but these few observations are made here simply to illustrate the application of the fragility test procedure.

Test data could be analyzed further to evaluate bushing response, but these few observations are sufficient to illustrate the application of CEFAPP. There are also other potential modes of failure that may not even be associated with the equipment's first mode of vibration. Many additional observations can be made about modes of failure from fragility test data, revealing additional information about the nature of equipment response and vulnerability. Fragility testing also may be used to evaluate methods of upgrading vulnerable equipment.

Probability Considerations for Fragility Data

The fragility data shown in Figure 13b are failure points for only one narrow-band random sweep record (Ran3, that has been scaled, HP filtered and notched). Other narrow-band random sweep records would create somewhat different failure data. However, one can assume failure is primarily due to a resonant response of some portion of the equipment. Equipment response is then similar to that of the response of a SDOF oscillator, from which response spectra are calculated. A single failure point on the TRS is the response of a SDOF oscillator, with the center frequency attributed to failure and the damping for which the response is calculated. Therefore, a different narrow-band random signal, scaled to produce the same equipment failure/response would generate a similar response of a SDOF oscillator at the frequency of failure, resulting in a failure point of essentially the same magnitude and frequency as that from the original record.

Real world equipment response will differ somewhat from that of a SDOF oscillator especially for equipment modes of vibration with large damping. The response of equipment will also be somewhat load path dependent, especially if the equipment responds in a non-linear manner. If the equipment failure causes significant material or geometric non-linear response the modes of vibration and therefore frequency of failure will shift (normally decrease because of the reduced stiffness that damage causes). Such non-linear response will make the equipment response and fragility data path dependent. Modal testing should be conducted both before and after fragility testing to determine if there was a frequency shift at the modes of vibration responsible for failure.

In the case of the bushing, the frequencies shown in Table 4 did not shift, which confirms that the bushing failures did not cause permanent mechanical damage, and the bushing response was not path dependent. Because the primary bushing modes of vibration have very low damping (2.5 % in the longitudinal direction - see Table 4), the bushing failure data from only one record is reasonable.

If other equipment being tested had greater damping or the failure modes included significant non-linear response, testing with multiple narrow-band random sweep record may be necessary. In the case of significant non-linear response, a new undamaged (or original one with the damaged components replaced) equipment specimen would need to be tested with the new narrow-band random sweep record.

Variations in equipment construction may lead to variation in the fragility data, if the modes of failure are influenced by properties of the equipment that vary. For example, if a failure mode is very dependent on a particular welded connection, then large tolerance in weld construction or variations in the quality of the weld will lead to large variation on the resulting fragility. This condition would require the testing of several specimens in order to build a statistically significant fragility data set. From this data confidence bands or probability of failure lines (drawn across the response spectra data envelope) would be added to the fragility data. The bushing failure leakage and slippage is dependent on the flange detailing, porcelain details at this connection, gasket construction and tension in the spring loaded center tension rod. It is assumed that all of these are standard for this model and manufacturer of bushing, with possible exception in the prestress of the tension rod. Therefore, it must be understood that the fragility data presented here is only applicable for the particular bushing tested and the user of such data would need to investigate if their bushing varies (in the construction related to the failure modes) from the one tested here. Again, it must be emphasized that this fragility test is only intended as a demonstration of CEFAPP and such details of the bushing construction had not been gathered.

Using the Fragility Data

The fragility data collected in the narrow band random sweep tests define the capacity of the equipment tested. Site-specific or IEEE 693 design spectra define the demand. Equipment vulnerability is determined by comparing the capacity and demand. For example, Figure 16 shows the bushing fragility data (capacity) together with a site-specific and IEEE 693 spectra (two cases of demand). The fragility data plots above the site-specific spectrum, indicating the bushing is not vulnerable to this seismic demand. However, the fragility data plots below the IEEE 693 spectrum between 4 and 7 hertz, indicating predicted failure to this seismic demand. In a similar manner the bushing capacity may be compared with other site-specific or design spectra. As noted previously, the IEEE 693 spectrum in Figure 16 should be modified to reflect transformer amplification. If the demand spectra plots above the fragility data (capacity), then the equipment is vulnerable to the type of failure that the fragility data represents (i.e., bushing fluid leaking and slippage in the current example).

Equipment vulnerability is defined as that region on the spectrum plot where the demand exceeds the capacity. Multiple regions may define more than one mode of failure, induced either by different failure mechanisms (e.g., leaking, slippage, or porcelain fracture) or different modes of vibration (e.g., 1st or 2nd lateral). Defining the vulnerability will guide equipment retrofit approaches.

If equipment fails qualification tests, CEFAPP can also be used as a diagnostic procedure to define the mode(s) of failure that prevented passing the qualification tests. The information gathered on mode of failure and amplitude and frequency of failure can be used to design a retrofit that will ensure the equipment passes the qualification test requirements.

Quantifying equipment dynamic characteristics and modes of failure is essential to developing equipment protection. Analytical models can be based on the vulnerability data gathered to allow the generalization of the vulnerability data to equipment with similar dynamic characteristics and modes of failure. Vulnerability of equipment not tested could be defined on the basis of such models.

3 Conclusions

This report demonstrates CEFAPP, an innovative equipment fragility test procedure developed by USACERL using the Triaxial Earthquake and Shock Simulator (TESS). The application of CEFAPP defines equipment vibration capacity with respect to frequency, which is compared to vibration demand in terms of design spectra to establish equipment vulnerability. The procedure was demonstrated as applied to a large power transformer bushing. Validation tests support the accuracy of this procedure for defining the capacity of equipment. The failure envelopes developed using this procedure can effectively be compared with seismic demand, thereby reducing the need for additional testing for unanticipated seismic hazards. This is especially true if demand is defined by site-specific spectra, because earthquake potential is then expressed in terms of its frequency content. Equipment vulnerability for various locations may be evaluated by comparing various site-specific spectra with the capacity spectrum defined by the original fragility testing, thus eliminating need for further testing to accommodate new or unanticipated demands.

The characterization of equipment vulnerability obtained by this test procedure provides essential guidance for equipment retrofit and new design improvements. This characterization also may be used to develop analytical models that would allow the generalization of the vulnerability data to equipment with similar dynamic characteristics and modes of failure. These models would define the vulnerability of equipment without conducting separate, dedicated tests.

Figures Referenced in Main Body of Report



Figure 1. TVA power transformer bushing tested on the USACERL TESS.

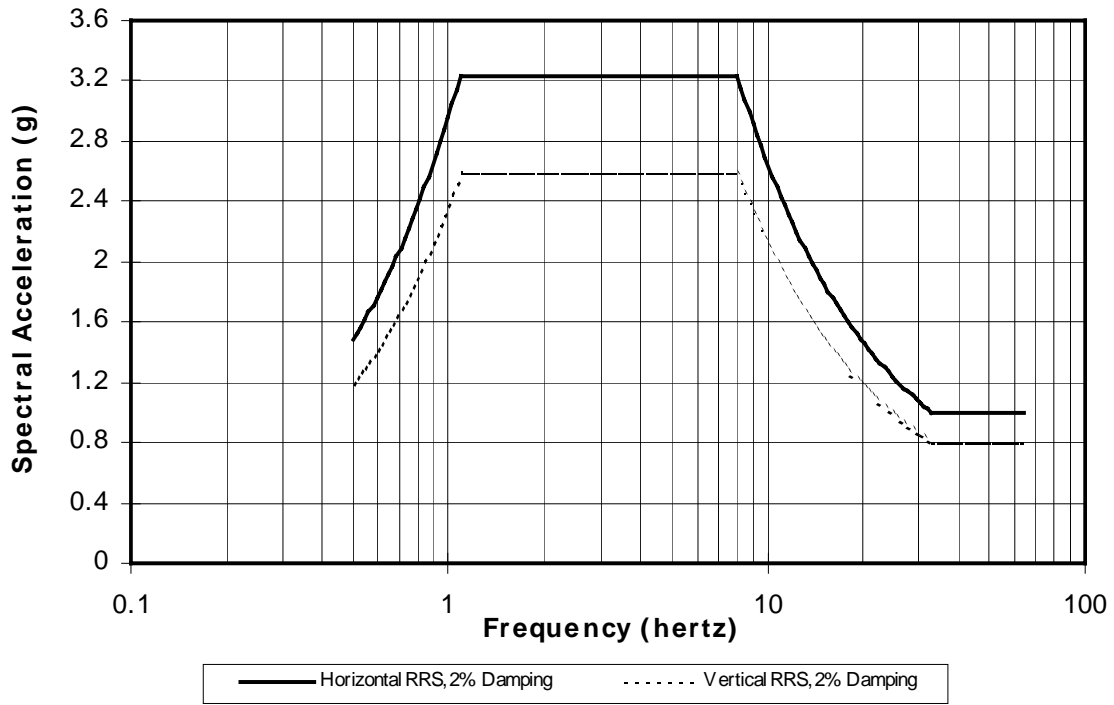


Figure 2. Horizontal and vertical response spectra, high seismic performance level, IEEE 693.

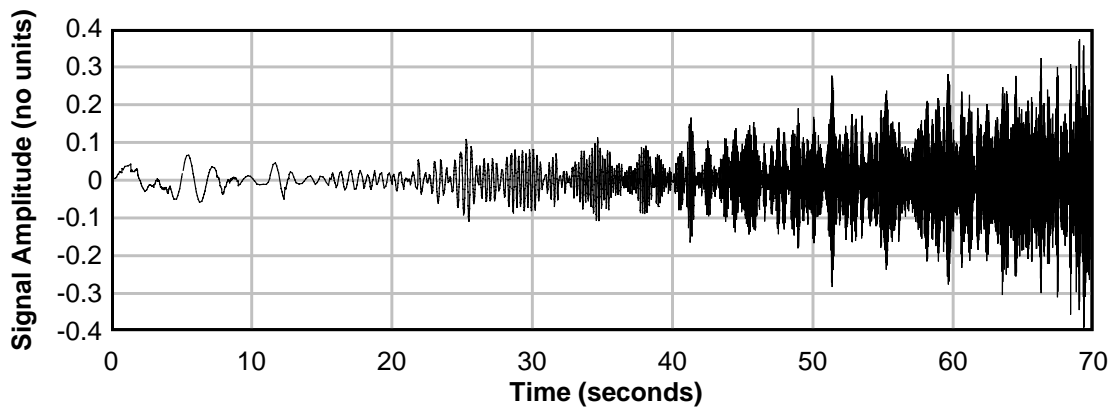


Figure 3a. Generated narrow-band random signal, Ran1.

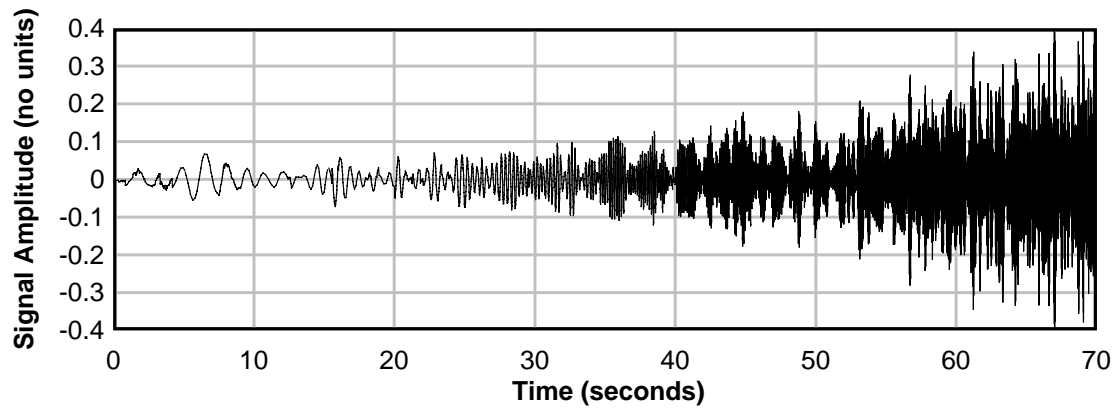


Figure 3b. Generated narrow-band random signal, Ran2.

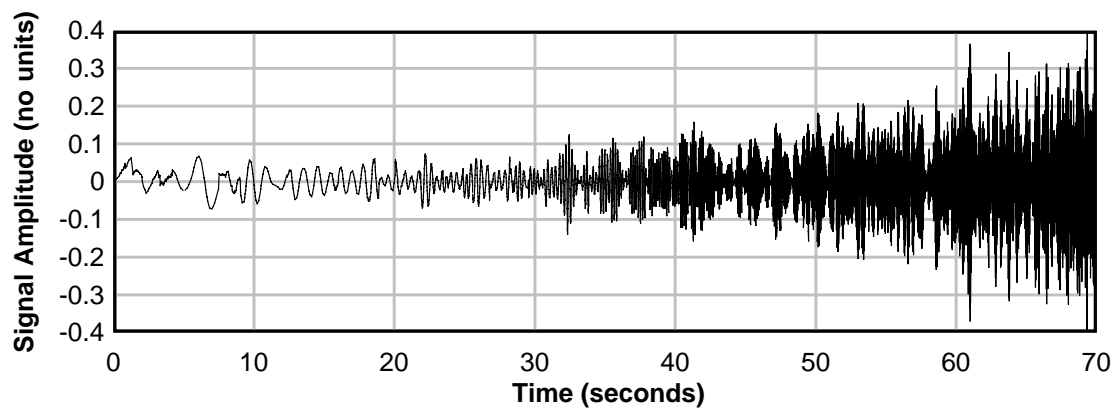


Figure 3c. Generated narrow-band random signal, Ran3.

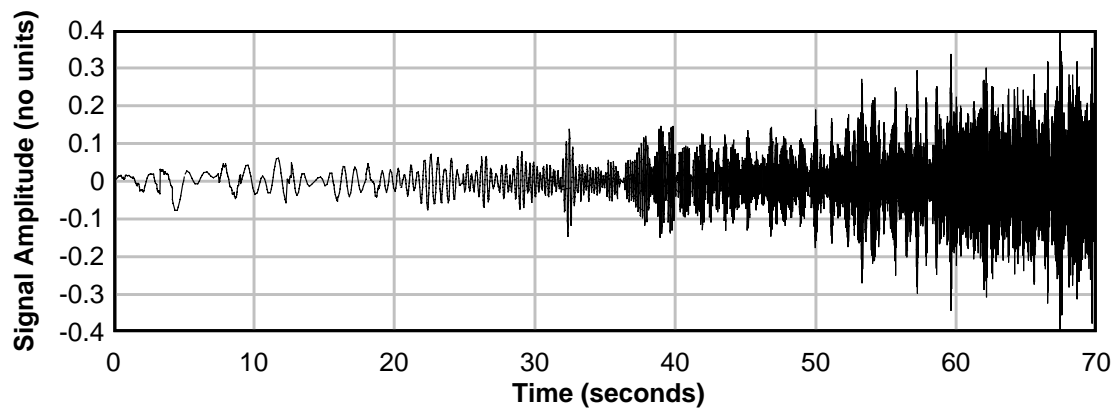


Figure 3d. Generated narrow-band random signal, Ran4.

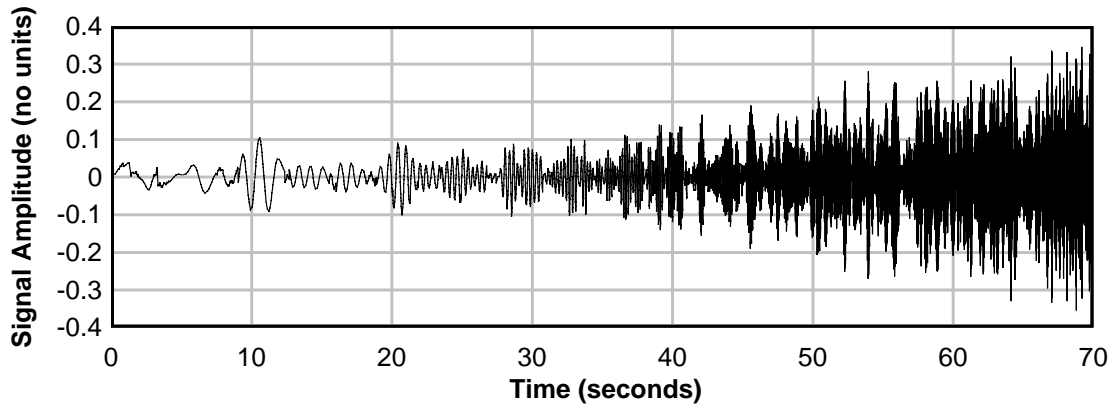


Figure 3e. Generated narrow-band random signal, Ran5.

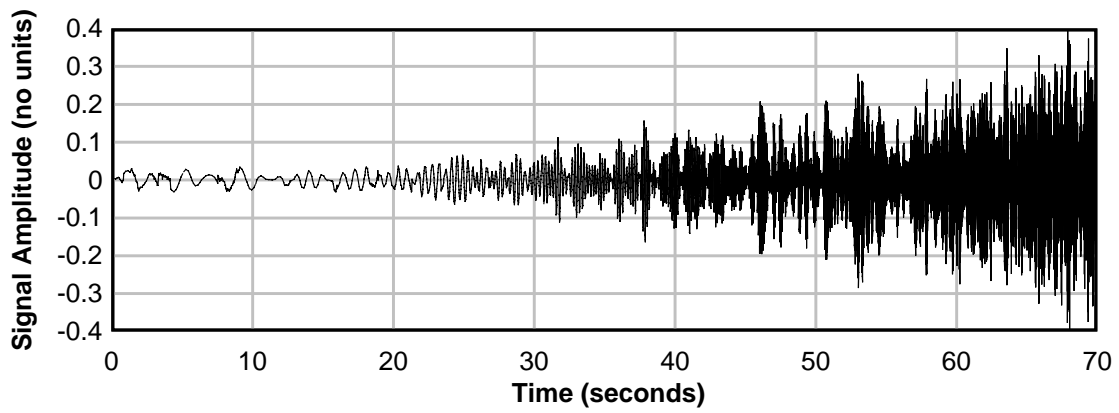


Figure 3f. Generated narrow-band random signal, Ran6.

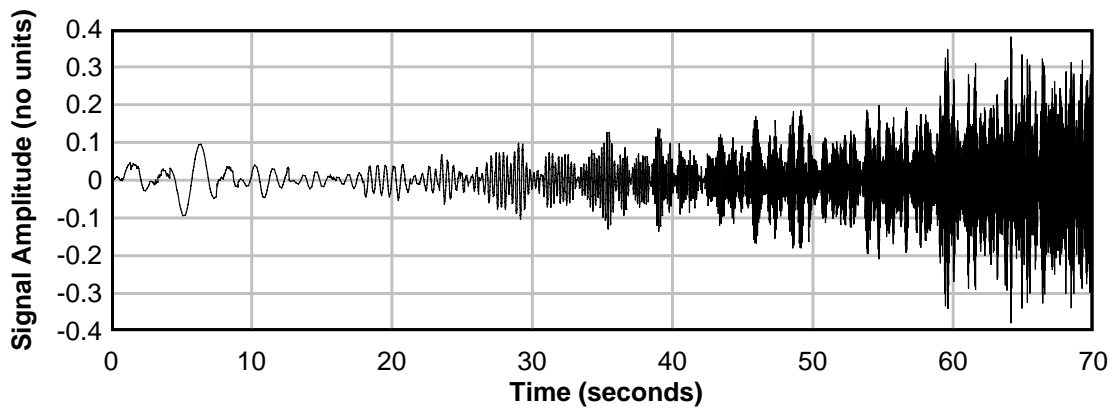


Figure 3g. Generated narrow-band random signal, Ran7.

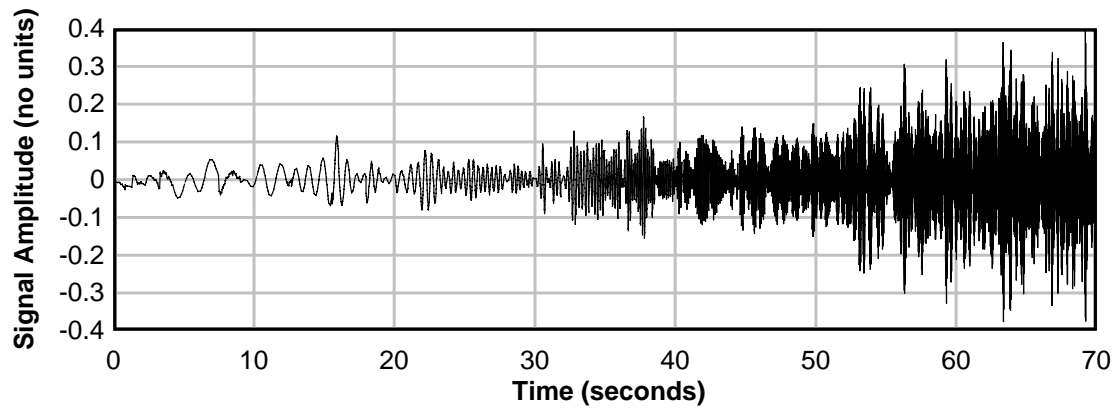


Figure 3h. Generated narrow-band random signal, Ran8.

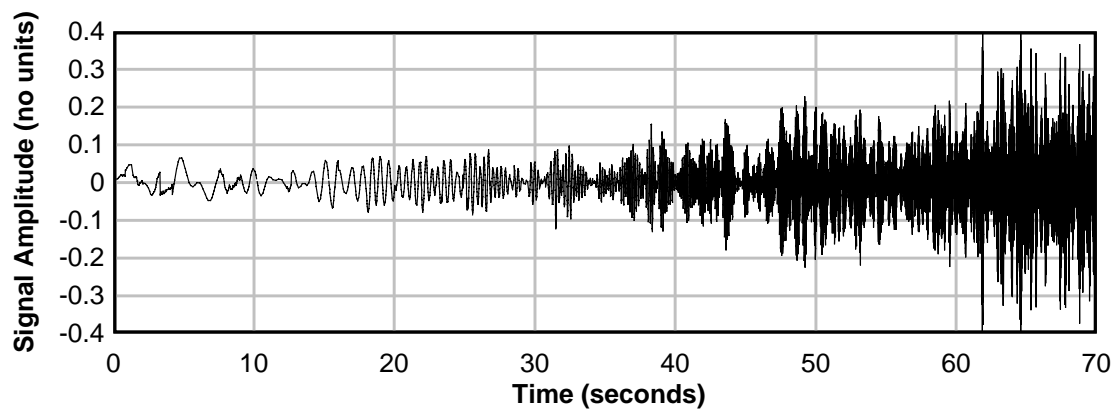


Figure 3i. Generated narrow-band random signal, Ran9.

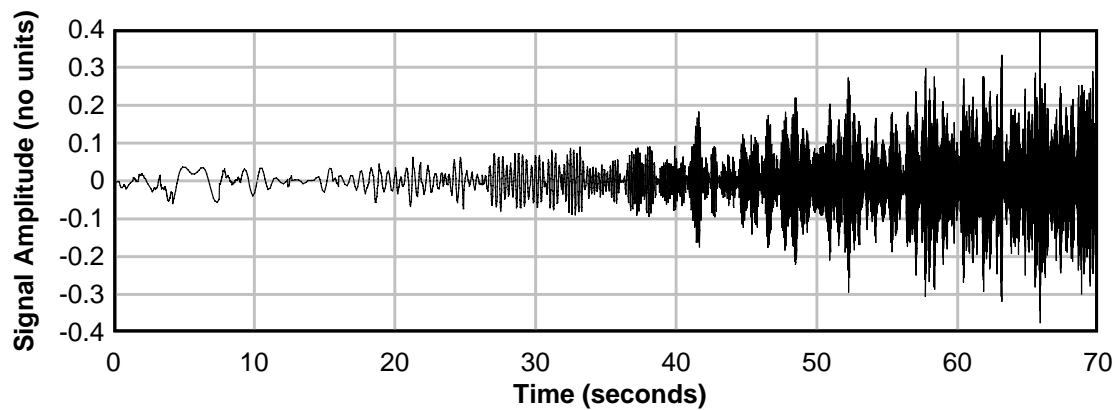


Figure 3j. Generated narrow-band random signal, Ran10.

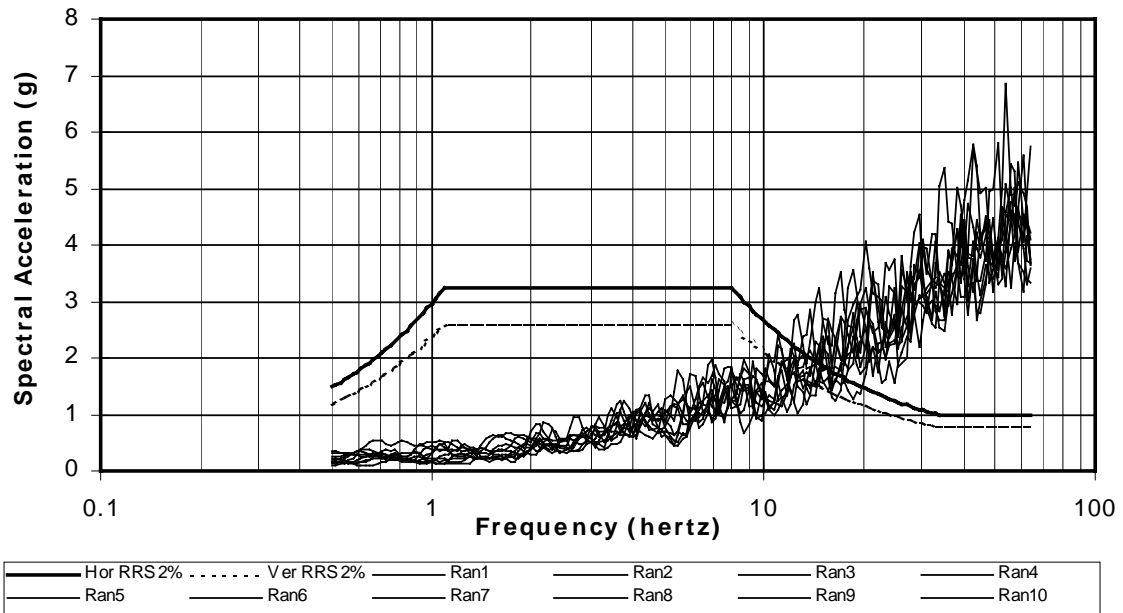


Figure 4. IEEE 693 high seismic performance response spectra and unscaled response spectra.

Scaling Relationships for Narrow-Band Random Tests

Frequency Range, $f_{n-1} - f_n$ (Hz)	Time Range $t_{n-1} - t_n$ (seconds)	Scale Number & Amplitude,		Horizontal Scaling, S_H (g)	Vertical Scaling, S_V (g)
		n	A_n (g)		
		0	12		
0.5 – 1.122	0 – 11.67	1	8	$\frac{A_1 - A_0}{t_1 - t_0}(t - t_0) + A_0$	$0.8 S_H$
1.122 – 8	11.67 – 40	2	2	$\frac{A_2 - A_1}{t_2 - t_1}(t - t_1) + A_1$	$0.8 S_H$
8 – 33.903	40 – 60.833	3	0.25	$\frac{A_3 - A_2}{t_3 - t_2}(t - t_2) + A_2$	$0.8 S_H$
33.903 – 64	60.833 – 70	4	0.2	$\frac{A_4 - A_3}{t_4 - t_3}(t - t_3) + A_3$	$0.8 S_H$

Note: This information is from Table 2 of this report.

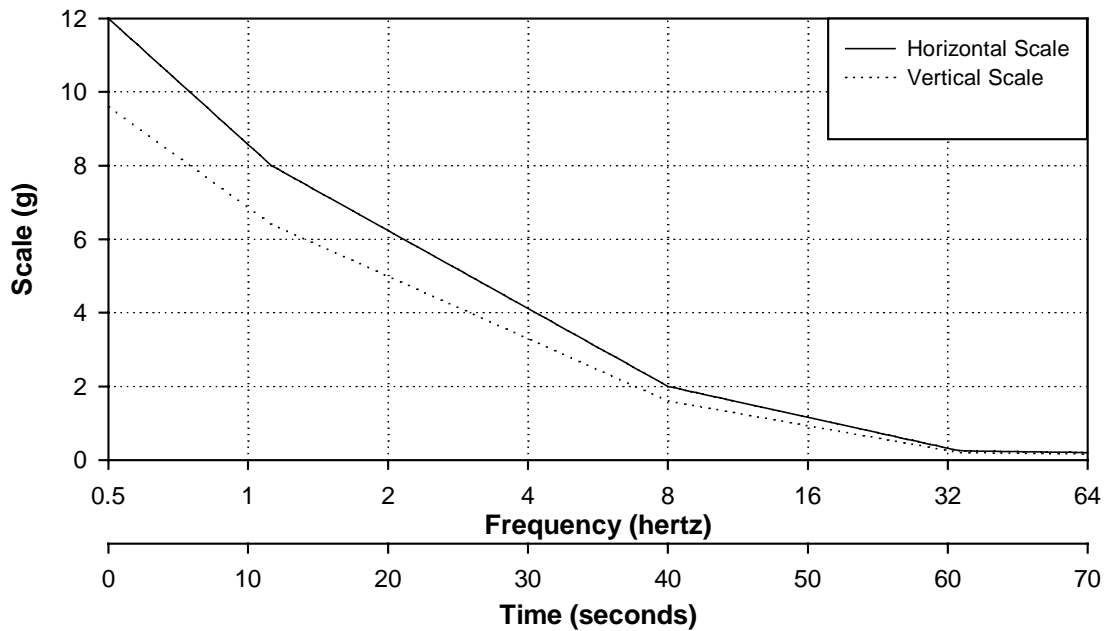


Figure 5. Scaling used for both horizontal (lateral and longitudinal) and vertical records.

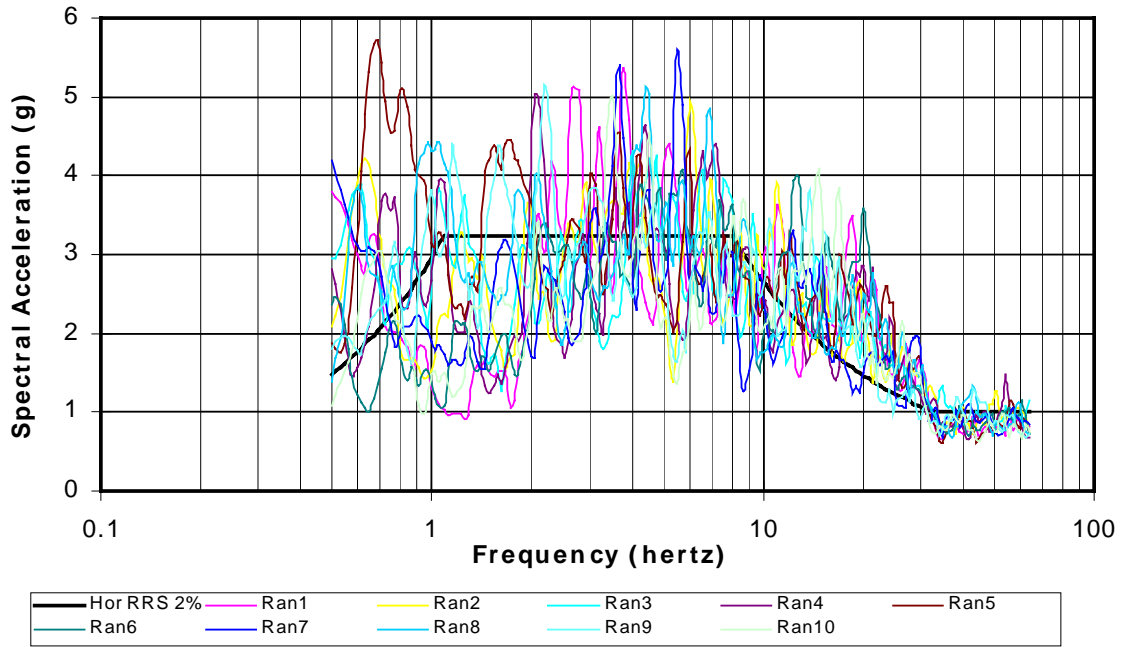


Figure 6a. IEEE 693 high seismic performance response spectra and scaled response spectra.

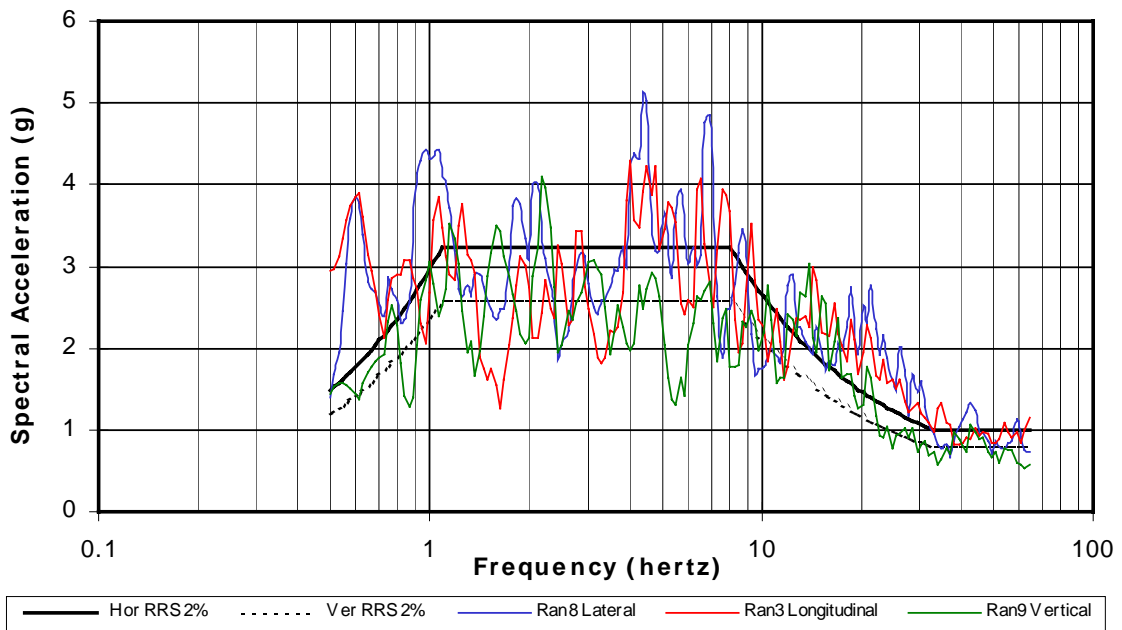


Figure 6b. IEEE 693 spectra and selected scaled response spectra.

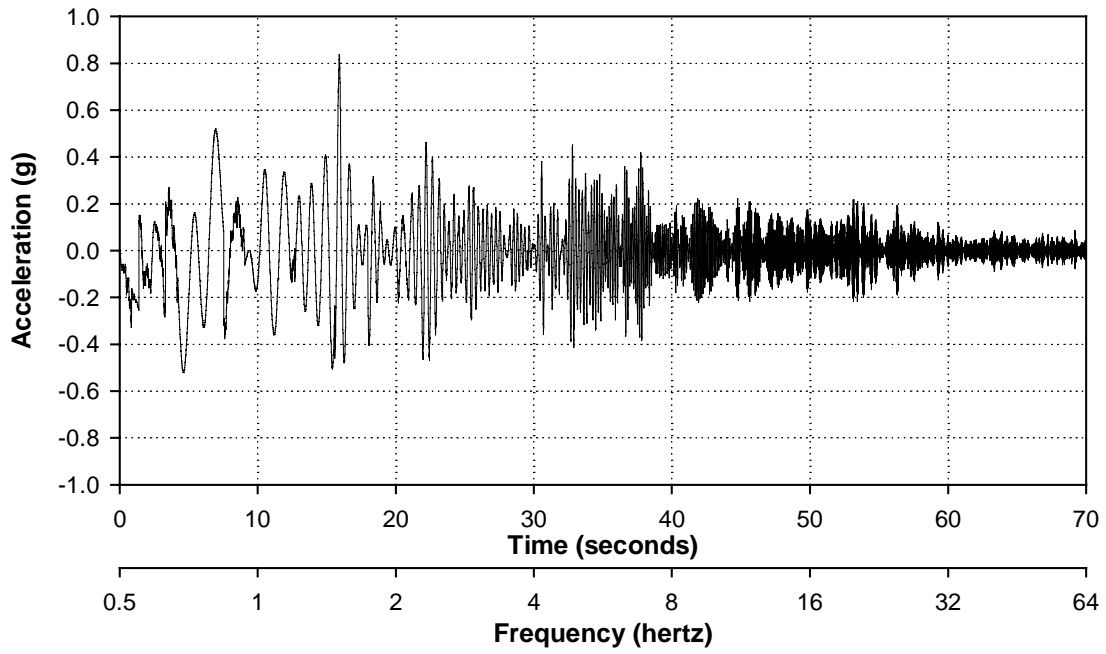


Figure 7a. Lateral narrow-band random scaled signal, Ran 8.

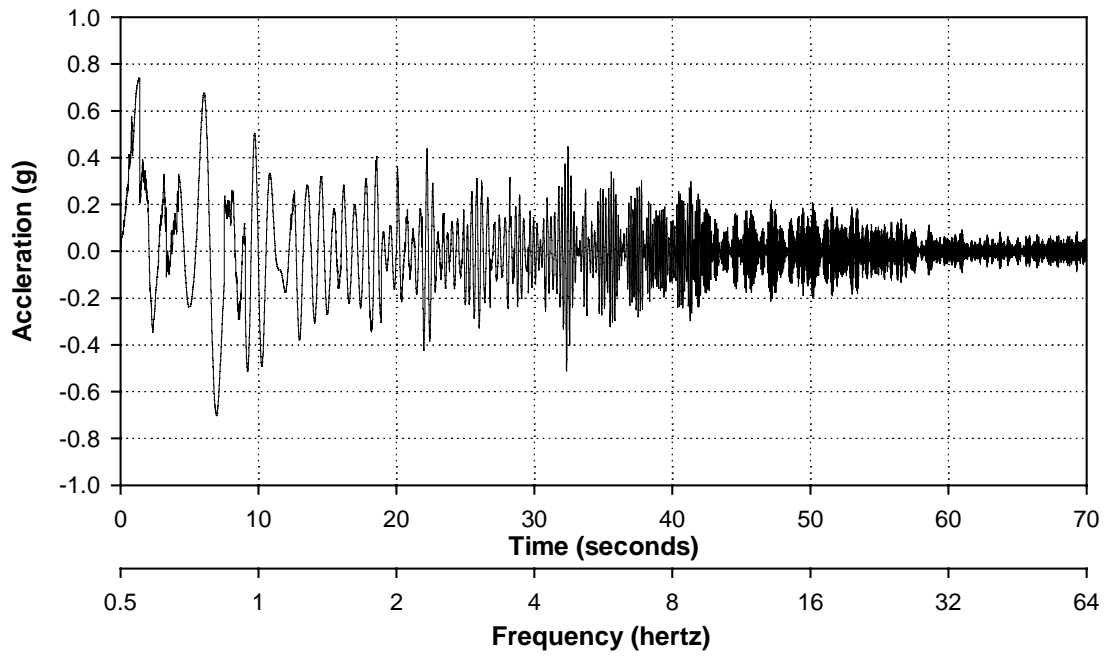


Figure 7b. Longitudinal narrow-band random scaled signal, Ran3.

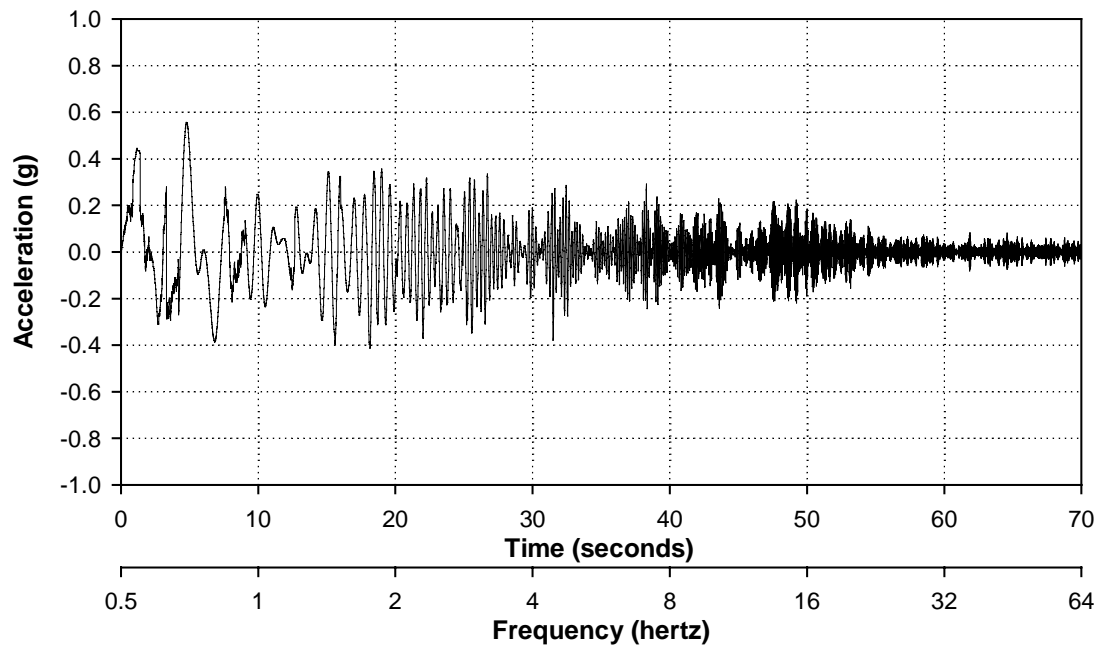


Figure 7c. Vertical narrow-band random scaled signal, Ran9.

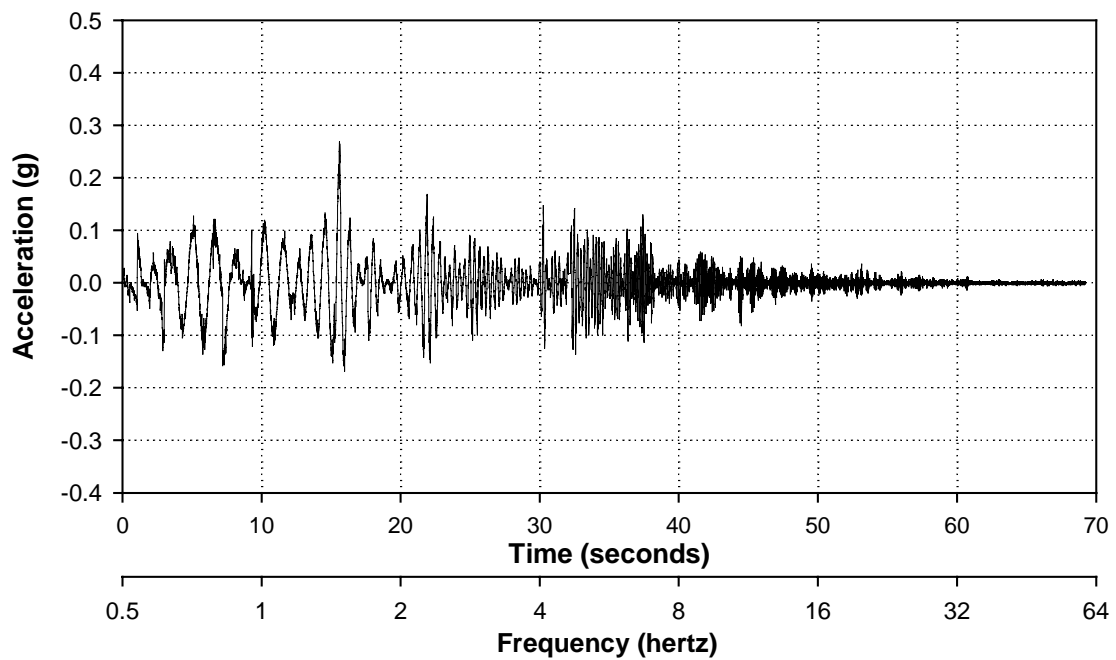


Figure 8a. Achieved lateral acceleration with input motions at 29% of Figure 7a.

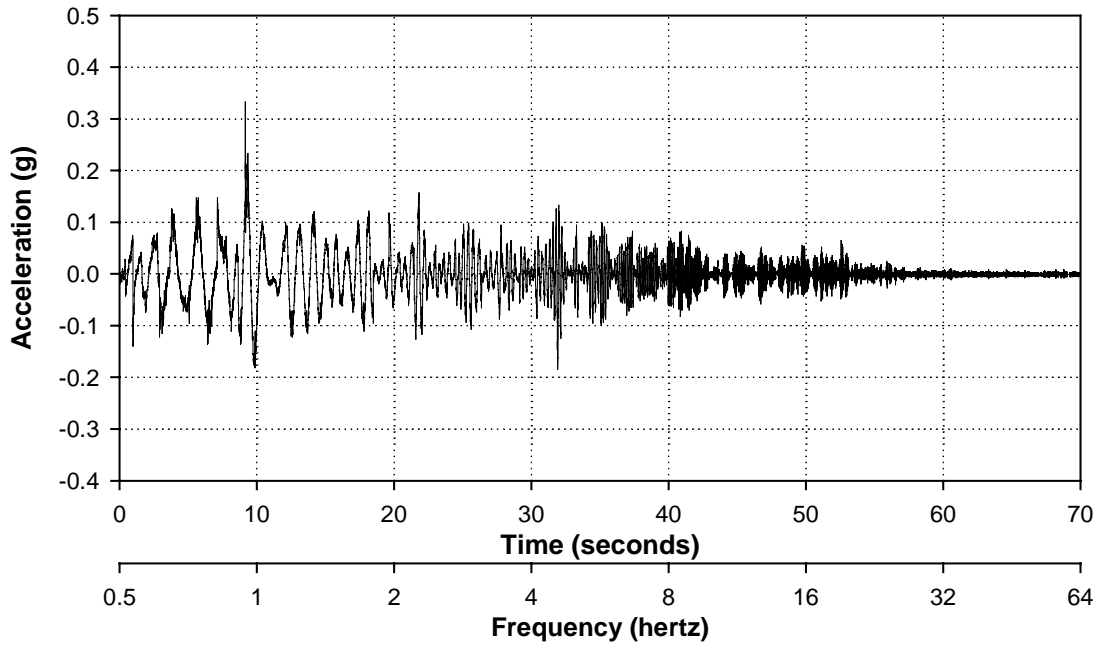


Figure 8b. Achieved longitudinal acceleration with input motions at 29% of Figure 7b.

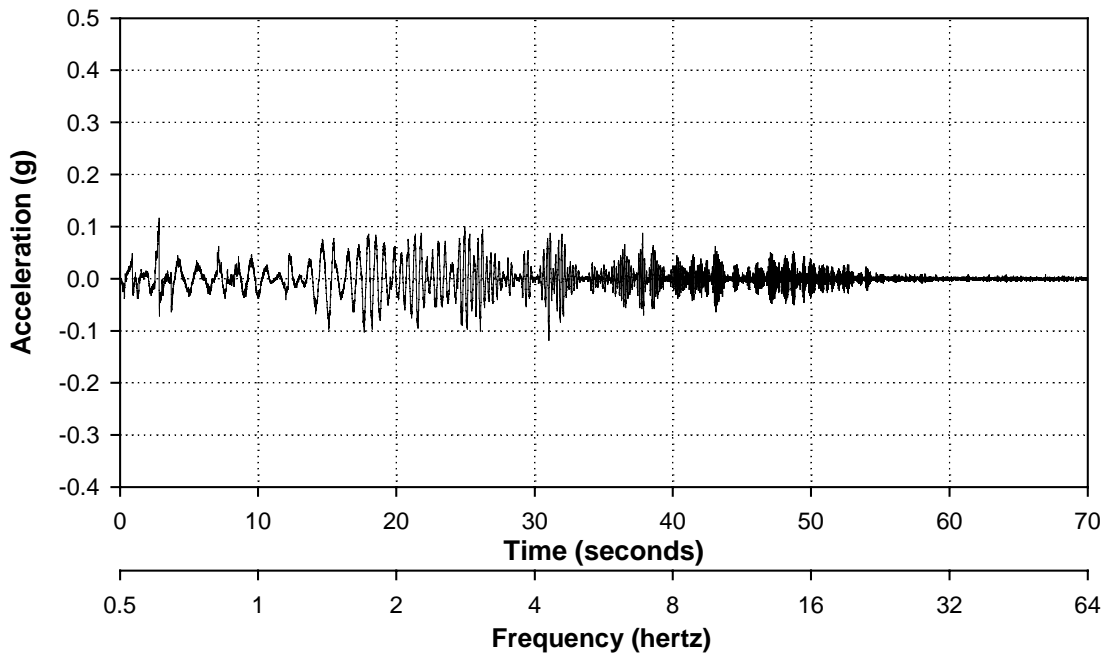


Figure 8c. Achieved vertical acceleration with input motions at 29% of Figure 7c.

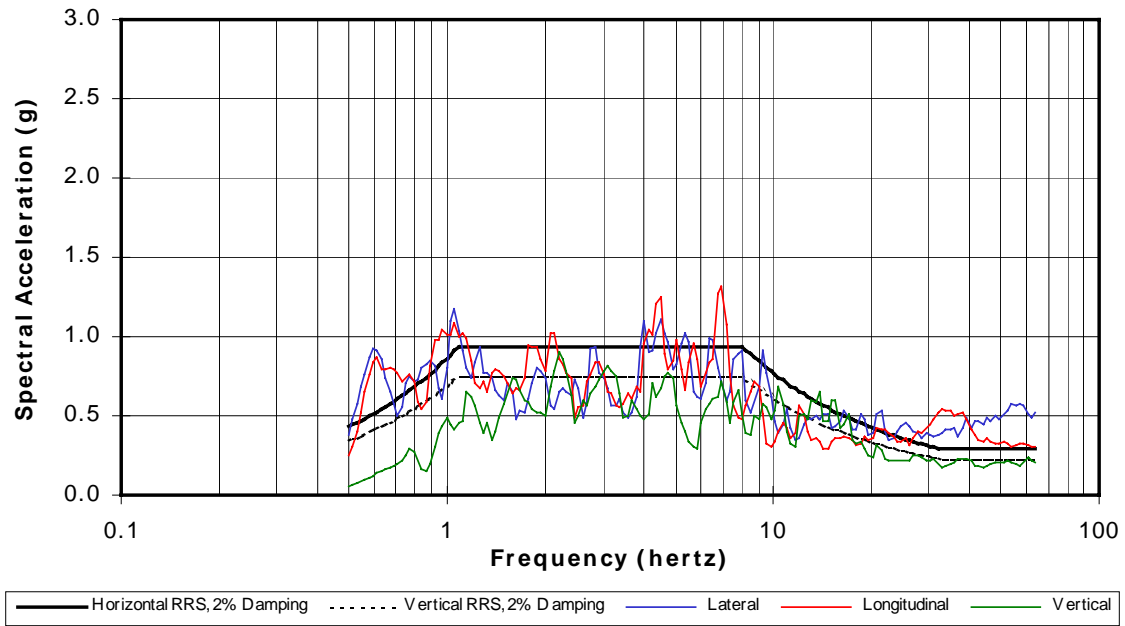


Figure 9. Test response spectra from 29% Figure 7 motions and 29% IEEE 693 spectra.

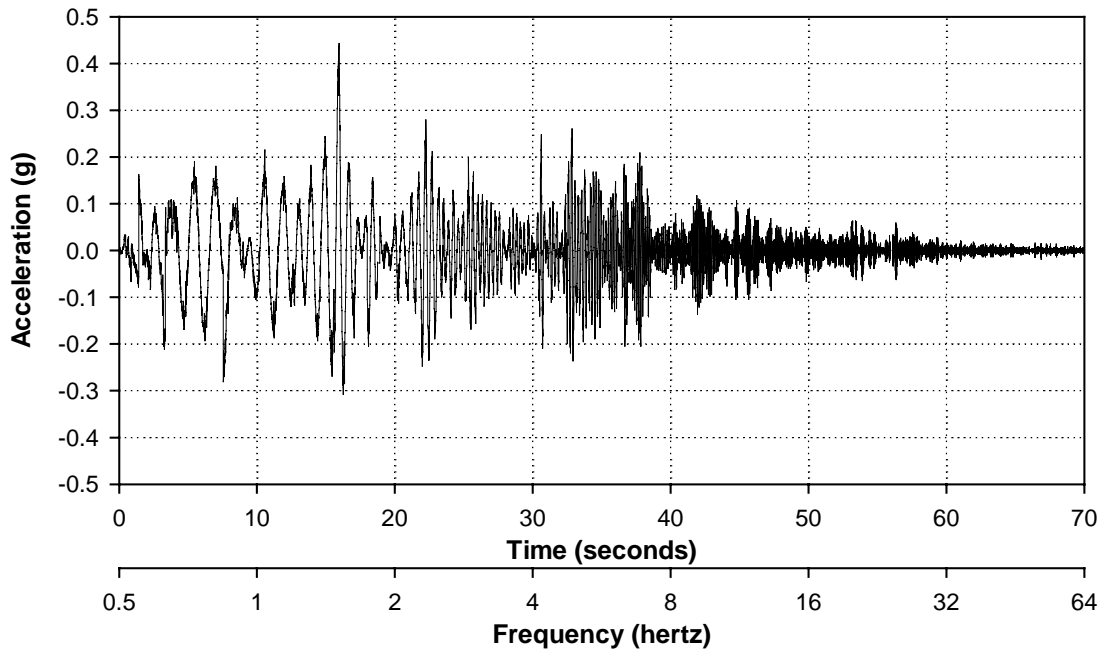


Figure 10a. Achieved lateral acceleration, 50% of Figure 7a (Frag10).

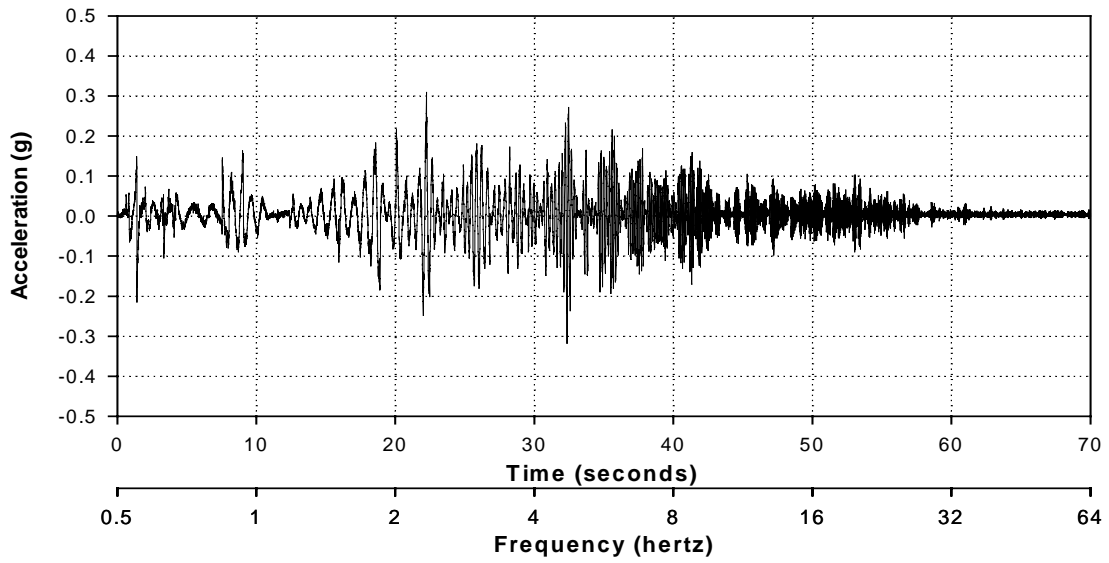


Figure 10b. Achieved longitudinal acceleration, 50% of Figure 7b with 1.2hz HP Filter.

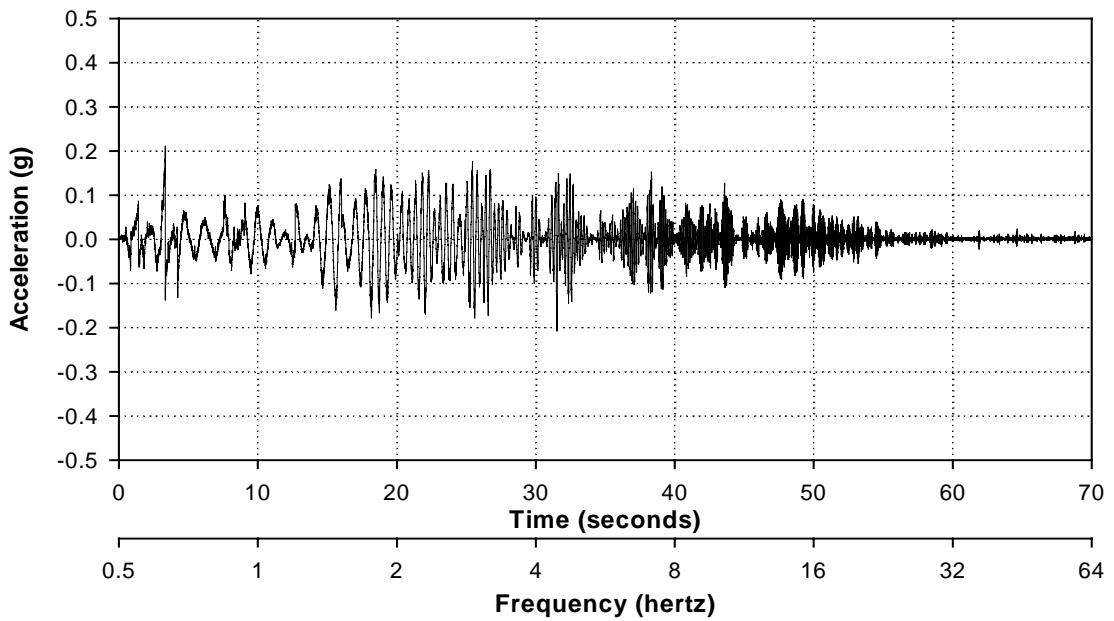


Figure 10c. Achieved vertical acceleration, 50% of Figure 7c.

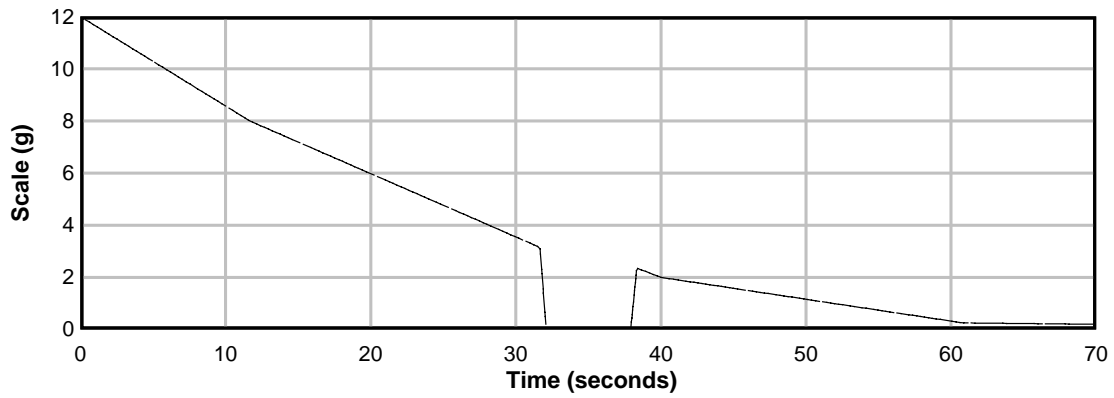


Figure 11a. Scale with Notch 2.

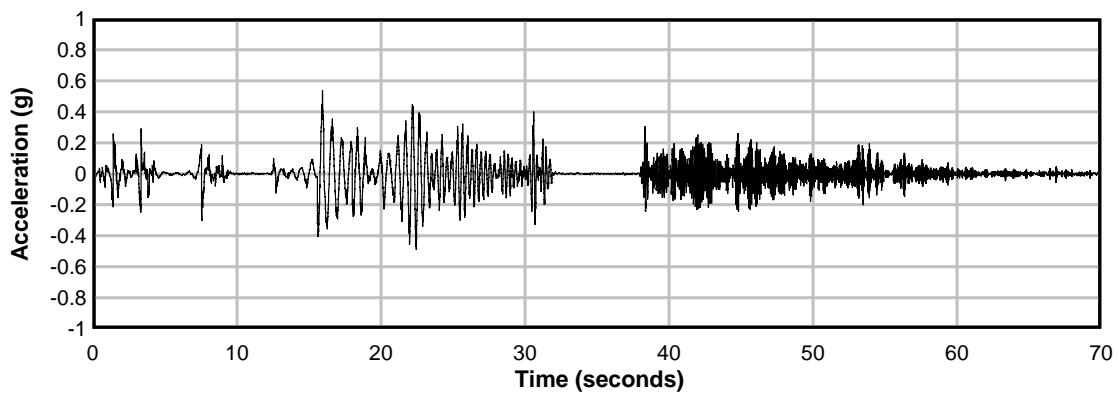


Figure 11b. Lateral achieved acceleration with Notch 2 and 100% of Figure 7a (Frag17).

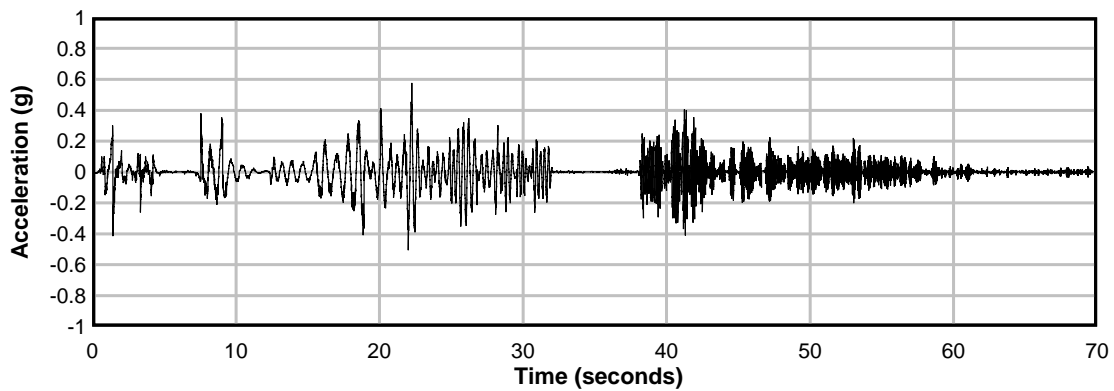


Figure 11c. Longitudinal achieved acceleration with Notch 2 and 100% of Figure 7b (Frag17).

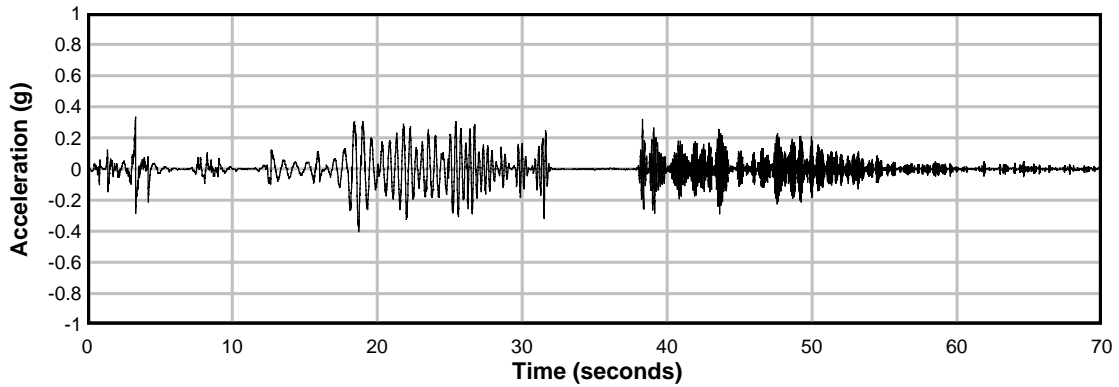


Figure 11d. Vertical achieved acceleration with Notch 2 and 100% of Figure 7c (Frag17).

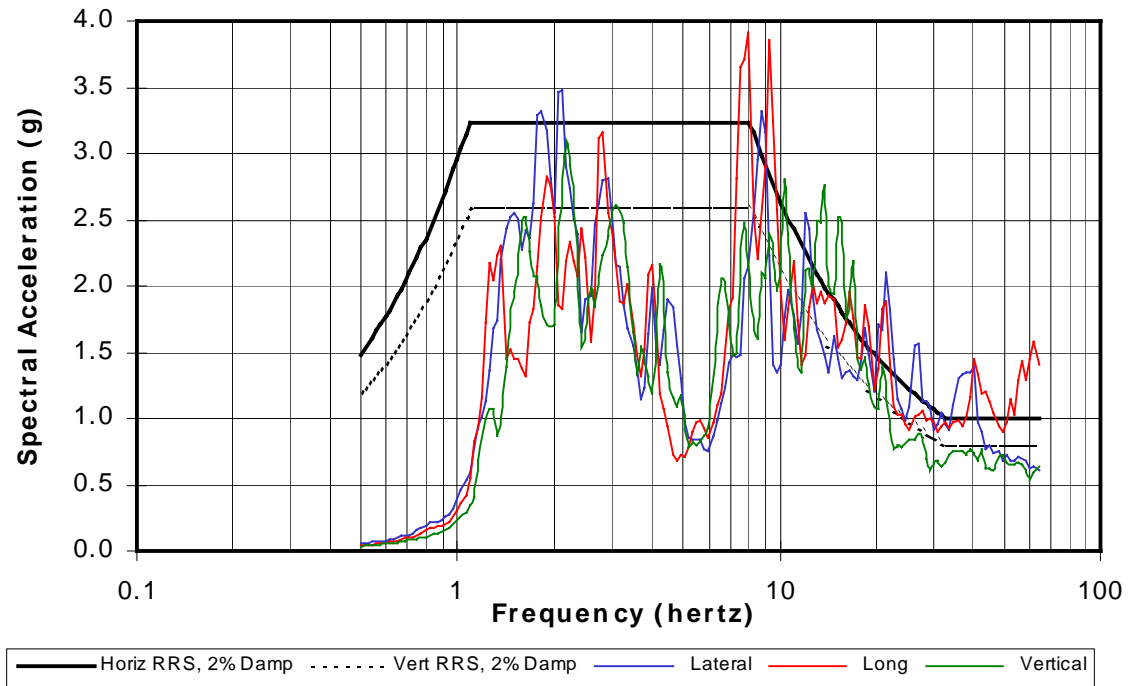


Figure 11e. IEEE 693 spectra and TSR for 100% of Figure 7 motions with Notch 2 (Frag17).

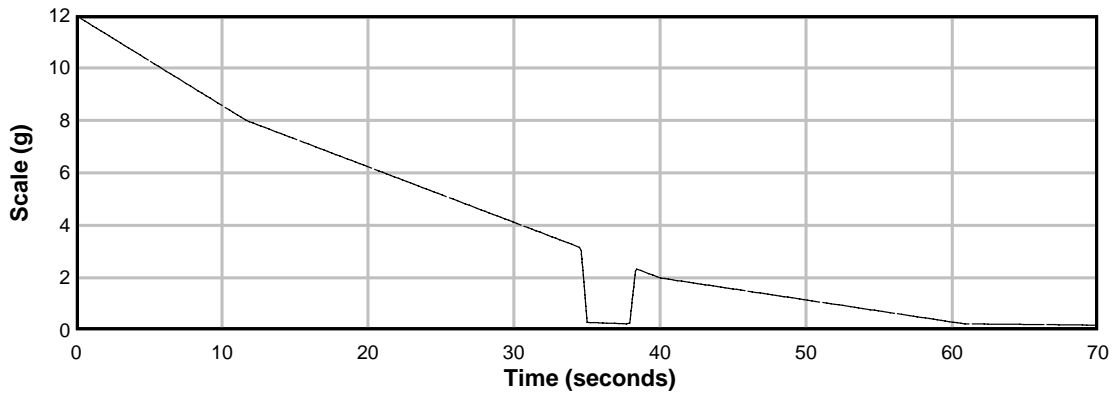


Figure 12a. Scale and Notch 1.

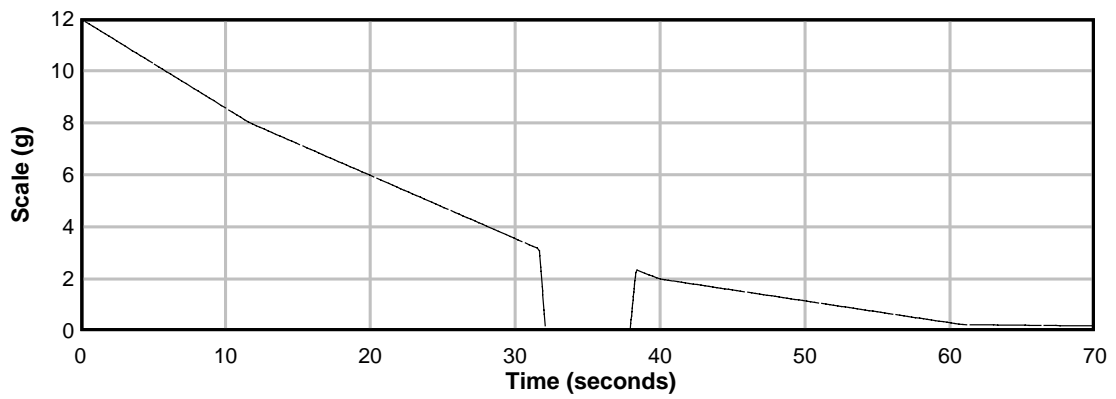


Figure 12b. Scale and Notch 2.

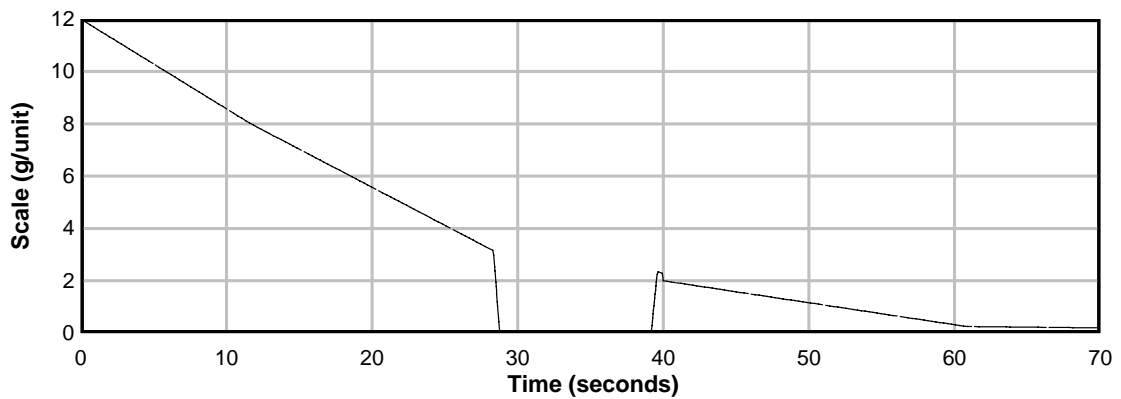


Figure 12c. Scale and Notch 3.

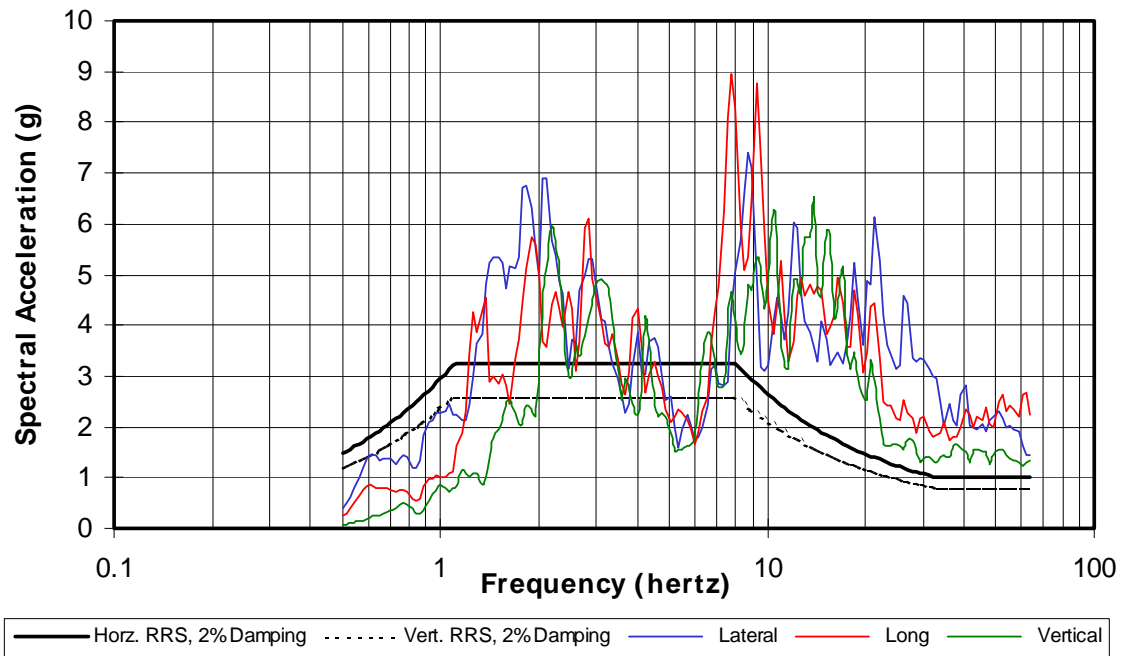


Figure 13a. Maximum TRS through Frag23, 220% of Figure 7.

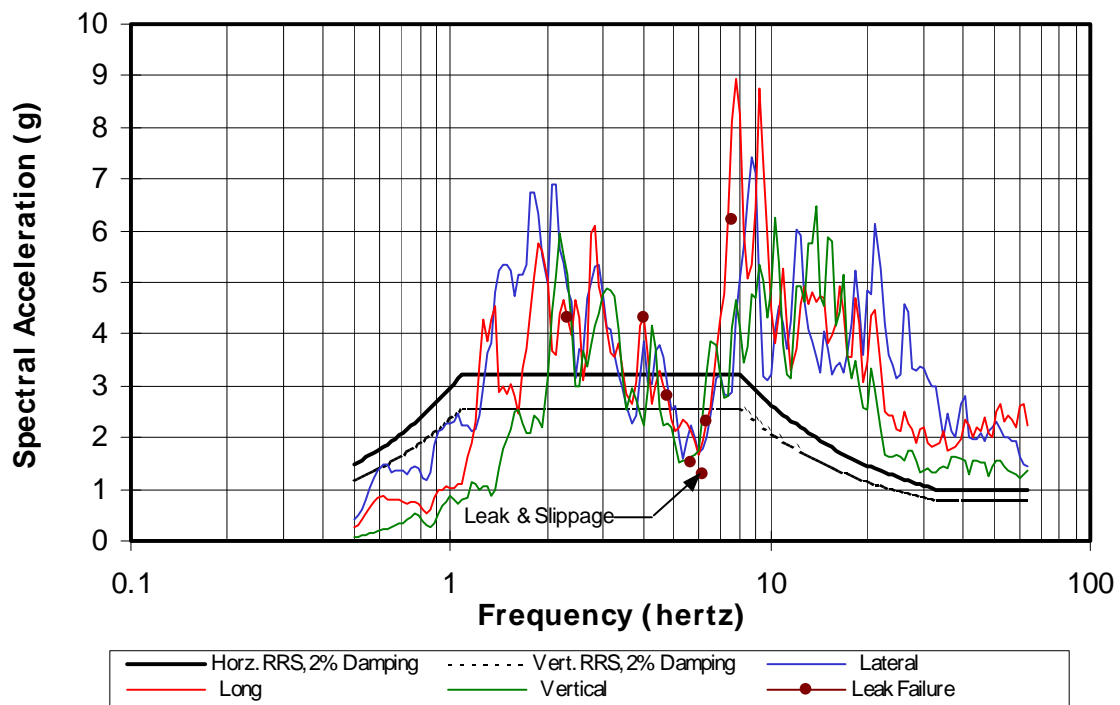


Figure 13b. Maximum TRS through Frag23 and failure data.

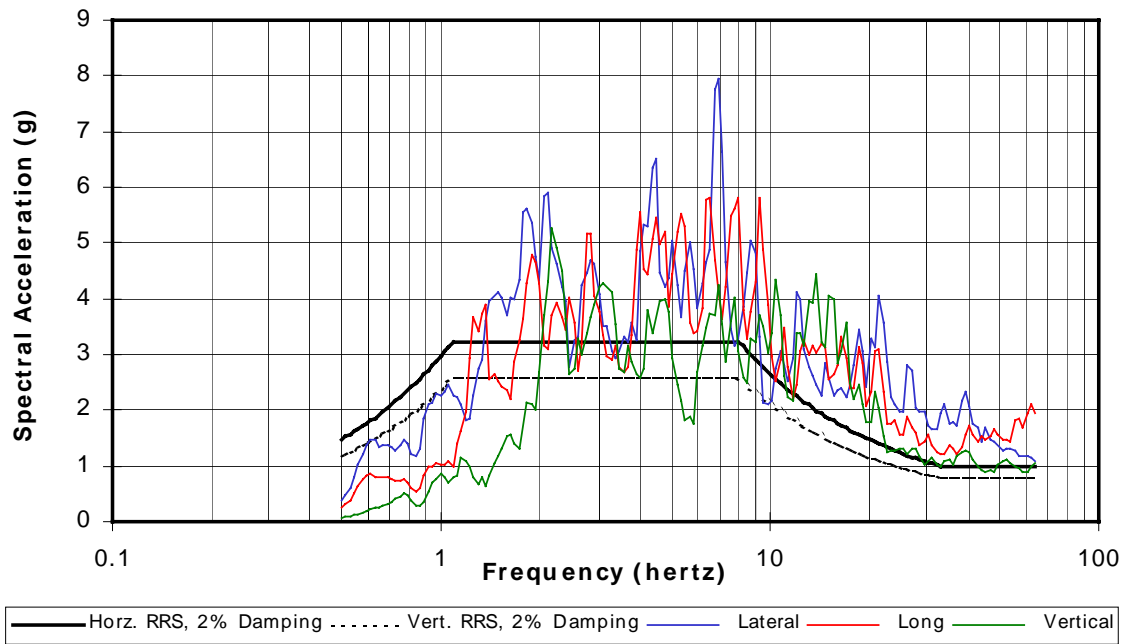


Figure 13c. Maximum TRS without notches.

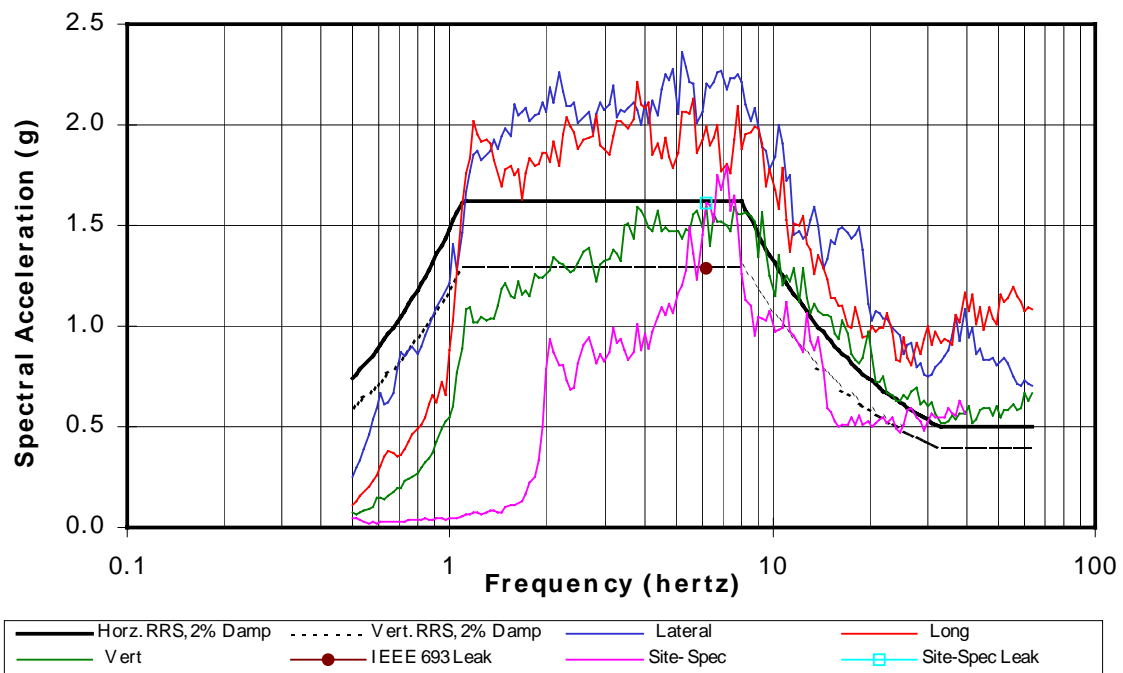


Figure 14a. IEEE 693 (at 50% PL) and site-specific spectra, TRS, and leak failures.

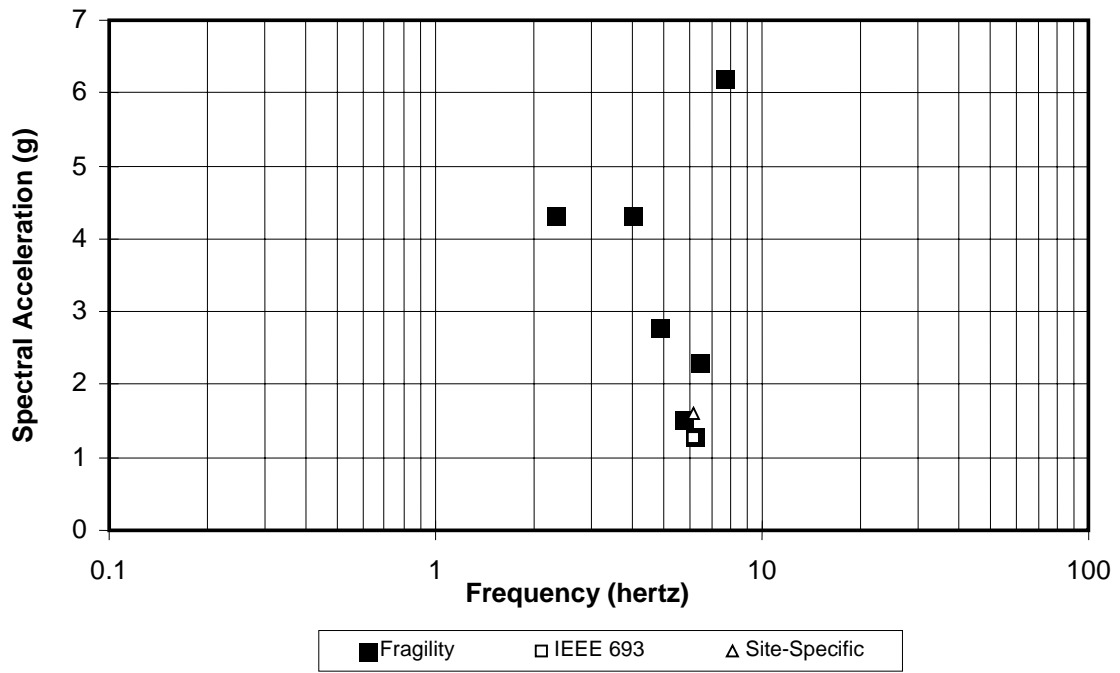


Figure 14b. Failure data from CEFAPP, IEEE 693, and site-specific tests.

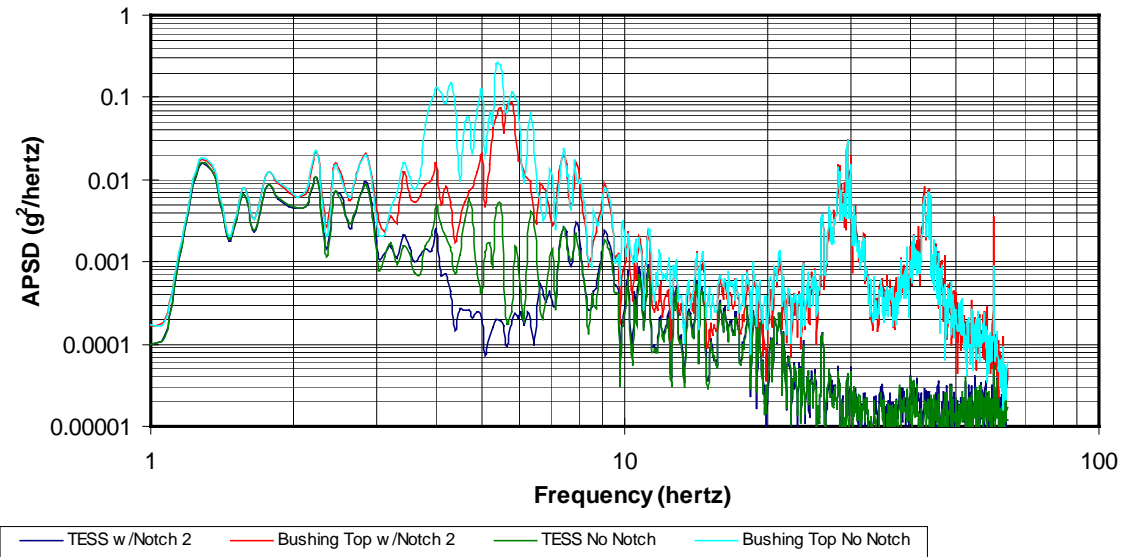


Figure 15. Acceleration power spectral density plots, longitudinal for 160% of Figure 7.

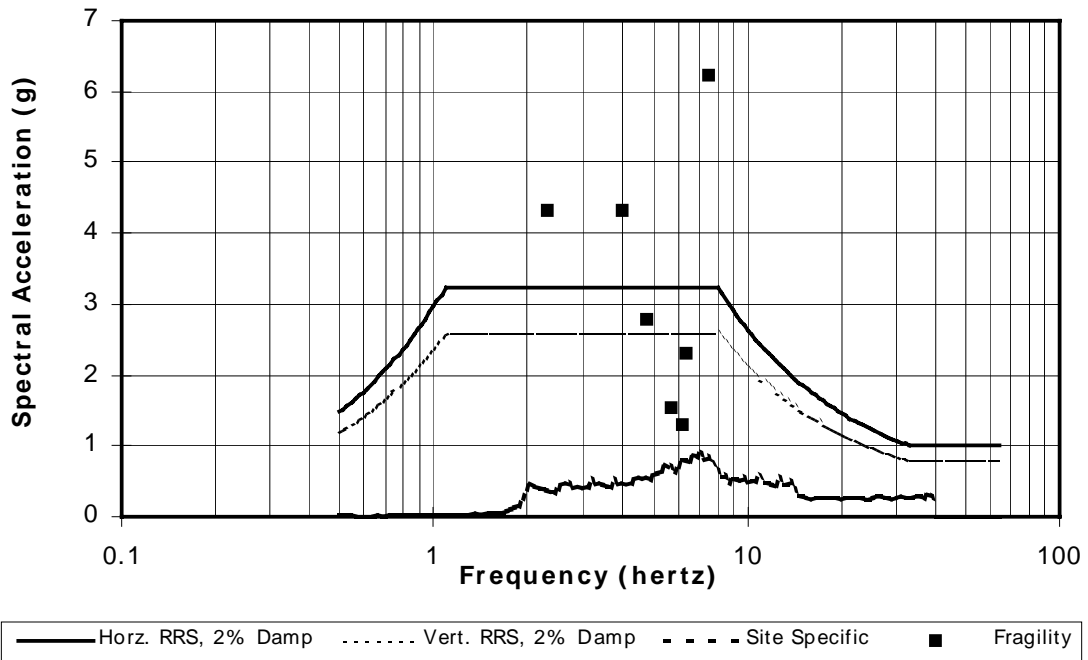


Figure 16. Fragility data with site-specific and IEEE 693 design response spectrum.

Appendix: Matlab Routine for Generating Narrow-Band Random Sweep Records

Narrow-band random signals, with a logarithmically increasing center frequency, were generated digitally using the *Matlab* routine RANSWP.M. Subsequent to this application an improved routine was developed. It is presented in Appendix A of USACERL Technical Report 97/58.

Requested input for this routine is:

kern: the current time (entered as *hour.minute*) is used as a kernel for the pseudo-random number generator. Unless otherwise instructed, the *Matlab* routine “rand” is initiated with the same number each time, thus always generating the same series of normally distributed “random” numbers. Initiating the routine with the current time is an effort to ensure the creation of unique random series.

aqrate: the sample rate (in hertz) at which the input signal should be created.

swrate: the rate (in octaves per minute) at which the center frequency is swept from its minimum to maximum value.

centerlow: the beginning center frequency (Hz).

centerhigh: the ending center frequency (Hz).

band: the filter bandwidth, in octaves.

outfile: the name of the output file in which to store the generated signal.

The algorithm for generating the test signal is outlined below.

A series of n random numbers is generated by

$$ran(i) = \sin(10\pi \times rand \times i), \quad i=1 \dots n.$$

This series is used to represent a time history of duration $n \div aqrate$ (sec), and will contain frequencies ranging from 0 Hz (though, in general, there will never be a DC component) to the nyquist frequency ($aqrate \div 2$). The sine was taken of the random numbers to alleviate problems that were encountered with spikes in the early, low frequency region of the record. Doing this does, however, alter the distribution of the random series from the default of gaussian. An improved method was developed and used in this routine for dealing with initial spikes, however the sine was also retained. In future records it is recommended to use the random numbers directly (i.e. $ran(i) = rand, i=1 \dots n$) so as to retain a gaussian distribution.

The primary loop of the routine generates the band pass filter and extracts the region of the record to be operated on. The logic of this loop is for increment i to represent the current point in time of the random series/time history by

$$t_i = \frac{i}{aqrate}.$$

A unique relationship is defined between time and frequency for these records allowing the current increment to also define the center frequency for the band pass filter as

$$\log f_i = \log f_{(min)} + \frac{\log(2)}{swrate} t_i$$

where f_{min} is the beginning center frequency (centerlow in ranswp.m). Knowing the center frequency and the filter bandwidth, at each new increment the band pass filter is updated. A simple filter was used that is a combination of two Heaviside step functions in the frequency domain. This can be defined before discretization as

$$h(f) = H(f - f_{low}) - H(f - f_{high})$$

where f_{low} and f_{high} are the upper and lower cutoff frequencies of the bandpass filter for iteration i , and the Heaviside functions are defined as

$$H(x - x_0) = \begin{cases} 0, & x < x_0 \\ 1, & x \geq x_0 \end{cases}$$

After creating this filter the region of the raw random signal that corresponds to the filter bandwidth (again equating time and frequency) is read into a separate vector for filtering. All filtering is carried out in the frequency domain by contracting the band pass filter with the inverse FFT of the extracted region of the random signal. Such a filtering algorithm can lead to numerical errors. Phase and magnitude distortion are not of particular concern in this application since the signal was random to begin with. Distortion of the frequency content of the filtered signal is of concern, however, power spectra analysis of the filtered record showed acceptable frequency response. After filtering, the data point corresponding to the current center frequency is stored in a separate vector along with all previous center frequencies and the loop is incremented.

At the completion of the main loop, an attenuation function that ramps from zero to unity is applied to one half of the first period of the filtered data. This was done to address the issue of an initial spike that was often experienced in the record and caused by a lack of rigorous enforcement of a zero initial value.

Finally, the vector *ranfiltm* is written to the output file (*outfile*).

The code for RANSWP.M is reproduced immediately below.

```
%          RANSWP.M

% Matlab M-file to calculate narrow band random signal
% based on a sweeping center frequency

% Request user input

kern = input('To initialize random number generator, enter time as
hr.min: ');
agrate = input('Enter the sample rate (Hz): ');
swrate = input('Enter the sweep rate (oct/min): ');
centerlow = input('Enter the beginning center freq. (Hz): ');
centerhigh = input('Enter the ending center freq. (Hz): ');
band = input('Enter the filter bandwidth (oct): ');
outfile = input('Enter the name of the signal output file: ','s');

% initialize random number generator

seed = round(kern^8)
rand('seed',seed)

% calculate system parameters: # octaves, duration, # data points

numoct = round((log10(centerhigh) - log10(centerlow))/0.30103)
```

```

time = numoct/swrate*60
npts = time * agrate

% Generate random series w/ unit amplitude

for n=1:npts
    ran(n) = sin(10 * pi*rand*n);
end

% MAIN LOOP for sweeping filter through random signal

    I=0;
    for I=1:npts

% bandtime and bandnum are the duration of and # data points
% in the bandwidth

        bandtime = 60*band/swrate;
        bandnum = round(bandtime*agrate);

% limits for the band pass filter, in terms of time (sec)
% and frequency (Hz)

        lowtime= I/agrate - bandtime/2;
        lowfreq = 10^(log10(centerlow)+(lowtime*swrate/60)*.30103);
        hightime = lowtime + bandtime;
        highfreq = 10^(log10(centerlow)+(hightime*swrate/60)*.30103);

% convert filter limits to number of data points to keep track
% of region of random series to be filtered

        lowpoint = round(agrate*lowtime);

% correction for lower band limit freq/time of early part of
% record defining a data point less than one, since low
% filter freq is less than the lowest freq in the record
        if lowpoint < 1
            lowpoint =1;
        end

        highpoint = round(agrate*hightime);

% equivalent correction for freq/time of the filter at the end of
% the record corresponding to # higher than actual # of data pts

        if highpoint > npts
            highpoint = npts ;
        end

% read in new portion of raw random series, equal in length to the
% filter band

```

```

    for j= 1:highpoint - lowpoint
        range(j) = ran(j+lowpoint);
    end

%
% generate simple filter based on heaviside functions where
% length(x) is the Matlab routine to return the size of vector x
%

    lim1 = round(lowfreq * length(range)/aqrates);
    lim2 = round(highfreq * length(range)/aqrates);
    lim3 = length(range);

    for p=1:lim1
        heavi(p) = 0;
    end
    for p=lim1:lim2
        heavi(p) = 1;
    end
    for p=lim2+1:lim3
        heavi(p) = 0;
    end

% filter present portion of random signal as contraction (vector
multiplication)
% of it's fourier transform w/ heaviside functions

    ftemp = fft(range);
    dummy = ftemp.*heavi;
    rantemp = ifft(dummy);

% add present filtered point to previously filtered region

    midpoint = round(bandnum/2) - 1;

% midpoint is a constant based on the # pts in the bandwidth.
% midpoint marks the midpoint of the vector rantemp, that temp-
% orarily holds the filtered region for the current increment
% Whereas lowpoint increases w/ each iteration as the filter
% sweeps through the record.

    if lowpoint < midpoint

% use this statement in early increments when length of rantemp
% is less than the length of the filter band

        ranfilt(I) = (rantemp(highpoint - midpoint))/(corr(I));
    else

% once the length(rantemp)=length(filterband) use this statement

```

```
        ranfilt(I) = (rantemp(midpoint))/(corr(I));

    end
% END MAIN LOOP
end

% attenuate 1/2 of beginning period to avoid initial spike

attentime = 1/(2*centerlow);
attenpts = attentime * agrate;

% initial ramp of attenuation function
    for I = 1:attenpts
        atten(I) = I/attenpts;
    end

% region constant unit magnitude
    for I = attenpts + 1: length(ranfilt)
        atten(I) = 1;
    end

    ranfiltm = atten.*ranfilt;

% write signal to file

fid = fopen(outfile,'w');
fprintf(fid,'%8.3f\r\n',ranfiltm);
fclose(fid);
```

USACERL DISTRIBUTION

Chief of Engineers	USA Natick RD&E Center 01760
ATTN: CEHEC-IM-LH (2)	ATTN: STRNC-DT
ATTN: CEHEC-IM-LP (2)	ATTN: AMSSC-S-IMI
ATTN: CECG	
ATTN: CECC-P	CEWES 39180
ATTN: CECC-R	ATTN: Library
ATTN: CECW	
ATTN: CECW-O	CECRL 03755
ATTN: CECW-P	ATTN: Library
ATTN: CECW-PR	
ATTN: CEMP	Defense Nuclear Agency
ATTN: CEMP-E	ATTN: NADS 20305
ATTN: CEMP-C	
ATTN: CEMP-M	Defense Logistics Agency
ATTN: CEMP-R	ATTN: MMBIR 22060-6221
ATTN: CERD-C	
ATTN: CERD-ZA	National Guard Bureau 20310
ATTN: CERD-L	ATTN: NGB-ARI
ATTN: CERD-M (2)	
ACS(IM) 22060	Naval Facilities Engr Command
ATTN: DAIM-FDP	ATTN: Facilities Engr Command (8)
	ATTN: Engrg Field Divisions (11)
CECPW 22310-3862	ATTN: Public Works Center (8)
ATTN: CECPW-E	ATTN: Naval Constr Battalion Ctr 93043
ATTN: CECPW-FT	ATTN: Naval Facil. Engr. Service Ctr 93043-4328
ATTN: CECPW-ZC	
US Army Engr District	8th US Army Korea
ATTN: Library (42)	ATTN: DPW (11)
	US Army MEDCOM
US Army Engr Division	ATTN: MCFA 78234-6000
ATTN: Library (8)	American Public Works Assoc. 64104-1806
US Army Engineering and Support Center	US Army CHPPM
ATTN: CEHND 35807-4301	ATTN: MCHB-DE 21010
US Army Europe	US Gov't Printing Office 20401
ATTN: AEAEN-EH 09014	ATTN: Rec Sec/Deposit Sec (2)
ATTN: AEAEN-ODCS 09014	
US Army Materiel Command (AMC)	Nat'l Institute of Standards & Tech
Alexandria, VA 22333-0001	ATTN: Library 20899
ATTN: AMCEN-F	Defense General Supply Center
	ATTN: DGSC-WI 23297-5000
FORSCOM	Defense Construction Supply Center
Forts Gillem & McPherson 30330	ATTN: DCSC-WI 43216-5000
ATTN: FCEN	
TRADOC	Defense Tech Info Center 22060-6218
Fort Monroe 23651	ATTN: DTIC-O (2)
ATTN: ATBO-G	
Fort Belvoir 22060	141
ATTN: CETEC-IM-T	(+40)
ATTN: CETEC-ES 22315-3803	11/97
ATTN: Water Resources Support Ctr	